JACOBS
UNIVERSITY

Randomized Network of Single Walled Carbon Nanotubes Thin Film Transistor: Fabrication, Simulation and Application as Biosensor

By

Sayed Alireza Mousavi

A Thesis submitted in partial fulfillment
of the requirements for the degree of

**Doctor of Philosophy in
Physics**

Approved Thesis Committee University of Salerno	Approved Thesis Committee Jacobs University Bremen
Prof. Vincenzo Tucci	Prof. Veit Wagner
Prof. Veit Wagner	Prof. Vincenzo Tucci
Prof. Giuseppe Milano	Prof. Jürgen Fritz
Prof. Danilo Roccatano	Prof. Patrizia Lamberti

Date of Defense:
28/10/2013

School of Engineering and Science

Contents

Abstract

Nanoelectronic devices based on nanomaterials, such as carbon nanotubes (CNTs) have attracted remarkable attention as a promising building block for future nanoelectronic circuits due to their exceptional electrical, mechanical and chemical characteristics. The electrical characteristics of CNTs, such as high mobility, quasi-ballistic conductance and resistance against electromigration, allow to surpass the properties of current Si based complementary metal oxide semiconductor (CMOS) devices. In particular, the large surface area and nanoscale structure makes SWCNTs promising candidates for chemical and biological sensing applications as well. Current research covers broad scientific fields, such as study of materials properties at nanoscale, development, fabrication and simulation of nanoscale structures, for electronics and biomedical applications. However, there is ample space for advancements in both theoretical studies and practical applications for CNT-based systems.

This thesis addresses the design and manufacture of thin film transistor (TFT) based on randomized network of single walled carbon nanotubes (SWCNTs) that exploit the unique properties of such materials to create a label-free biosensor for detection of variety biomolecules, particularly proteins. In addition, in order to analyze the electric transport of SWCNTs network in the TFT channel a numerical 3-dimensional (3D) model for the thin film layer is developed.

The SWCNTs-TFTs are fabricated by using microfabrication to obtain a micro-interdigitated electrode (μ-IDE) as drain-source electrode. The sizes vary between 2 to 50 μm. Thin-film transistors (TFTs) are fabricated by using SWCNTs thin film as the semiconducting layer and SiO_2 thin film as the dielectric layer. The high purity semiconducting network of SWCNTs layer is deposited with an effective technique that combines the silanization of the substrate with vacuum filtration process from dispersed SWCNTs in surfactant solution. . The adopted technique provides a low-cost, fast, simple, and versatile approach to fabricate high-performance SWCNTs-TFTs at room temperature. The morphological arrangement of SWCNTs forming the active layer in the channel of the transistor is checked with scanning electron microscopic (SEM). The TFTs obtained exhibit p-type transistor characteristics and operate in

accumulation mode. The results are interpreted by considering the percolation theory. The exponent α of the power law describing the conductivity can be linked to the structural complexity of the SWCNT network. In particular an exponent $\alpha = 1.7$ was found experimentally, showing that the obtained thin film is relatively dense and near percolation. In addition, the experimental data have been compared with the results of the 3D model simulating the charge transport in the SWCNT structures formed in the TFT channel. The simulation results lead to an exponent $\alpha = 1.8$ that is in good agreement with the experimental data. The proposed model seems to be able to reliably reproduce the transport characteristics of the fabricated devices and could be an effective tool to improve the SWCNTs-TFTs structure. Moreover, the fabricated SWCNTs-TFT devices provide a suitable platform for high-performance biosensors in label-free protein detection. The sensing mechanism is demonstrated on a proof of principle level for the interaction of biotin and streptavidin on the SWCNTs surface. It is used as a research model for biosensor application. The SWCNTs thin-film biosensor has high sensitivity and it is capable of detecting streptavidin at concentration of 100 pM.

Motivation and Objective

Recently, low-dimensional materials have attracted great attention in the field of nanoelectronics for various applications e.g. integrated circuits (ICs) and sensing systems. Particularly, single walled carbon nanotubes (SWCNTs), due to exceptional electrical properties such as high mobility at room temperature are used for building nanoelectronic devices. Moreover, the large surface area and nano scale structure of SWCNTs makes them one of the most interesting materials for chemical and biological application.

Although a single carbon nanotube exhibits very high mobility, the fabrication of electronic devices such as field effect transistor (FET) based on carbon nanotubes is highly challenging and not technologically established for large area applications and scalable manufacturing devices. In addition, carbon nanotubes show heterogeneous electrical features such as mixture of metallic and semiconducting species. Moreover, they show different diameters and lengths. Furthermore, the synthesis carbon nanotubes require a high temperature environment which is not compatible with arbitrary substrate materials. To overcome these problems and meanwhile take advantage of such an exceptional nano-material, this work investigates the fabrication and electrical properties of thin film transistors (TFTs) based on randomized network of single-walled carbon nanotubes at room temperature. The devices are manufactured using a post-growth deposition technique. The fabricated SWCNTs thin film transistor is used as a transducer for bio-molecules detection, particularly as a label-free bio-sensor. The advantage of label-free bio-sensing compared to the labelled one is the fact that additional processes that can degrade sensitivity and alter the system response are avoided. Moreover, in order to investigate the electrical transport of SWCNTs network inside the channel of TFTs a 3D-numerical modelling is performed.

Bottom-gate TFTs were fabricated on a highly p-doped Si substrate with a thermally grown SiO_2 layer (100 nm) as a gate dielectric. The bottom source/drain electrodes in the form of interdigitated electrodes (IDEs) were fabricated by standard photolithography and lift-off processes. The feature sizes of the microstructures are varying between 2 to 50 μm. Subsequently, the thin film of SWCNTs is deposited with an effective technique that combines the silanization of

substrate with vacuum filtration process. High purity semiconducting SWCNTs are dispersed in surfactant solution and are deposited on the substrate with patterned electrodes. This technique provides a fast, simple, and versatile approach for fabrication of high-performance SWCNTs-TFTs at room temperature. The spatial arrangement in SWCNTs network was investigated by using a scanning electron microscope (SEM). The SWCNTs-TFTs exhibits p-type transistor characteristics. High purity semiconducting SWCNTs are used as an active layer in the channel of TFTs. They provide suitable platforms for high-performance biosensors. Particularly, functionalized SWCNTs surface with biotin is used to detect the protein, streptavidin (SA). The high purity semiconducting SWCNTs network has high sensitivity and it is capable of detecting SA at an ultra-low concentration of 100 pM.

In order to understand the transport properties of SWCNTs network, a numerical simulation has been developed using a 3D model. The channel of TFT structure is modelled as a random mixture of conducting cylinders. . The variation of electrical conductivity of the structure can be computed by implementing a 3D resistor network which includes resistors associated to the intrinsic resistance of SWCNTs and tunnelling effect between conducting clusters. By using a Monte Carlo analysis the behaviour of the electrical conductivity and the dependence of the percolation thresholds as a function of geometrical and physical influencing parameters can be analyzed. The results of numerical simulations are in good agreement with those obtained from the experimental characterization.

The research project carried out during the PhD program has been focused on three main aspects:

- Fabrication and electrical characterization of SWCNTs-TFTs.
- Development of an accurate numerical model which can be used to obtain information on the transport properties of randomized network of SWCNTs in the channel of TFT structure based on geometrical and physical properties of SWCNTs.
- Application of the SWCNTs-TFT as a transducer for a label-free biosensor for detection of a specific protein.

This thesis is organized as follows.

- In the first chapter a general overview on carbon nanotubes, properties, and the most promising applications of CNT is given.
- In the second chapter state of the art related to mechanisms of growing carbon nanotubes, experimental procedures to separate the semiconducting from metallic SWCNTs and various deposition technique are described.
- In the third chapter the fabrication procedure for making thin film transistor using a wet chemical of SWCNTs solution, the results concerning the electrical characterization on SWCNTs-TFTs containing different concentrations of semiconducting SWCNTs are described in detail. In addition, the morphological arrangement of SWCNTs network is investigated.
- Chapter 4 provides an overview on the models available in the literature and then presents the numerical model that has been implemented. A detailed description of the modelling of SWCNTs-TFT based on a 3-dimensional (3D) model, both in terms of geometric approach and the optimization algorithm is given. The simulation results obtained by such a model are provided and compared with the obtained experimental results.
- In chapter 5, the characteristic of the fabricated SWCNTs-TFT used as a transducer for high-performance label-free biosensors is presented. The biosensor is used for the detection of a specific protein, streptavidin (SA). In addition, the interaction between streptavidin and biotinylated SWCNTs surface of TFT structures is described.

- In chapter 6, conclusion and future work in this field are discussed.

Chapter 1

Carbon nanotubes: Properties and Structure

This chapter presents a general overview of carbon nanotubes (CNTs) and their unique characteristics which make them suitable materials for different applications and excellent candidates to form the active layer in the channel of a thin film transistor (TFT). The main forms and characteristics of CNTs, namely Single Walled (SWCNT) and Multi Walled (MWCNT) are presented. In particular, the electrical properties of CNTs, are illustrated.

1.1 Carbon Nanotube

1.1.1 Overview

The molecular carbon structures called carbon nanotubes (CNTs) were discovered by Japanese physicist Sumio Iijima in 1991 while performing transmission electron microscopy (TEM) experimental observation on fullerenes [1]. He produced carbon fibers by using an arc-discharge evaporation method. Those fibers grew at the negative side of the electrode and he observed that each fiber contained coaxial tubes of graphitic sheets in a helical fashion which are called multi walled carbon nanotubes (MWCNTs). In 1993, Iijima and Ichihashi [2] and Bethune *et al* at IBM [3, 4] independently produced single walled carbon nanotubes (SWCNTs) based on gas phase catalytic growth.

Because of their unique electrical, chemical and mechanical features [5-7], carbon nanotubes ,are highly required for mass production in future applications. Nowadays, there are various methods for the synthesis of large quantities of carbon nanotubes such as laser ablation

[8], chemical vapor deposition (CVD) [9-11], gas phase catalytic growth [12, 13], and arc discharge [1]. Among these methods the CVD technique is preferred because it enables the production of aligned CNT bundles and self-oriented CNT arrays [14].

1.1.2 Carbon nanotube structure: SWCNT & MWCNT

There are two types of carbon nanotubes because of their shapes, called single-walled carbon nanotubes (SWCNTs) and multi-walled carbon nanotubes (MWCNTs) [15] . The schematic of SWCNT and MWCNT is shown in Figure 1.

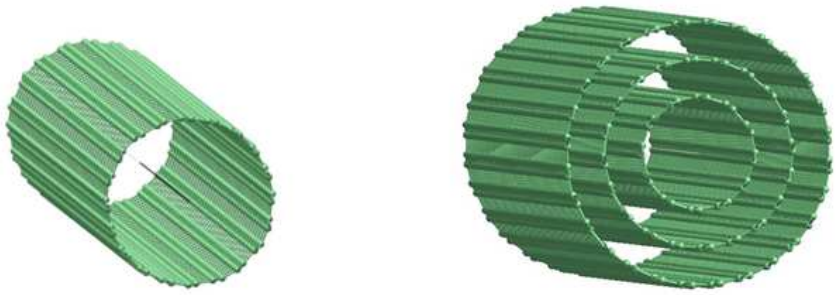

Figure 1. Schematic model of SWCNT and MWCNT. (structures were generated using GTK Display Interface for Structures GDIS 0.90.)

A single walled carbon nanotube (SWCNT) is considered as a hollow cylindrical nano-structure which is made by rolling of a graphene sheet (one atomic layer of graphite) [16]. The schematic of how a graphene sheet wraps to form SWCNT is shown in Figure 2. SWCNTs exhibit high length-to-diameter ratio with adiameter in the range of a few nanometers (0.5-5 nm) and lengths in the order of micrometers [17]. MWCNTs have the same structure as SWCNTs; however, being made of multiple concentric tubes, they show a diameter bigger than SWCNTs (range of 10 to 30 nm) [18]. The offends of a carbon nanotube (either SWCNT or MWCNT) are closed with a hemisphere shape of buckyball structure.

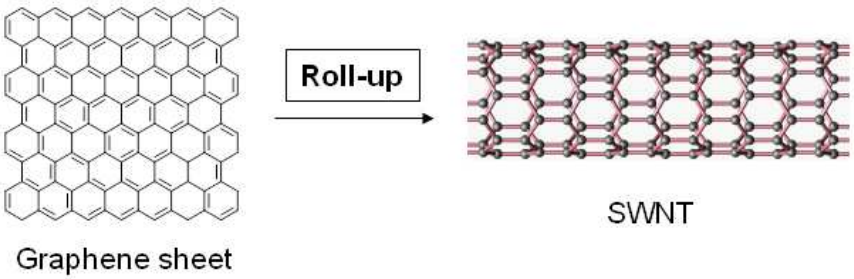

Figure 2. Wrapping of graphene sheet to form SWCNT

The physical features and electronic structure of SWCNTs are variable and depend on the geometry and how it is rolled up from graphene sheet [19]. These characteristics are important to know and enable scientists to gain knowledge about properties and performance of devices based on carbon nanotubes. The structure of SWCNT is defined by considering how it folds. The folding is described by a certain angle along the graphene sheet axis which is described by a chiral vector, $\vec{C}$, and a chiral angle, θ [20, 21]. As shown in Figure 3 the chiral vector is determined based on a_1 and a_2 as the unit vector along the X and Y direction of a two-dimensional (2D) graphene lattice respectively. Moreover, n and m are integers representing the numbers of repeating units along the two directions of graphene sheet. The chiral vector C_h is defined as [21] :

$$\vec{C} = na_1 + ma_2 \tag{1}$$

It is convenient to specify SWCNT with numbers (n, m). These integers uniquely determine the chiral angle and diameter of carbon nanotubes [21].

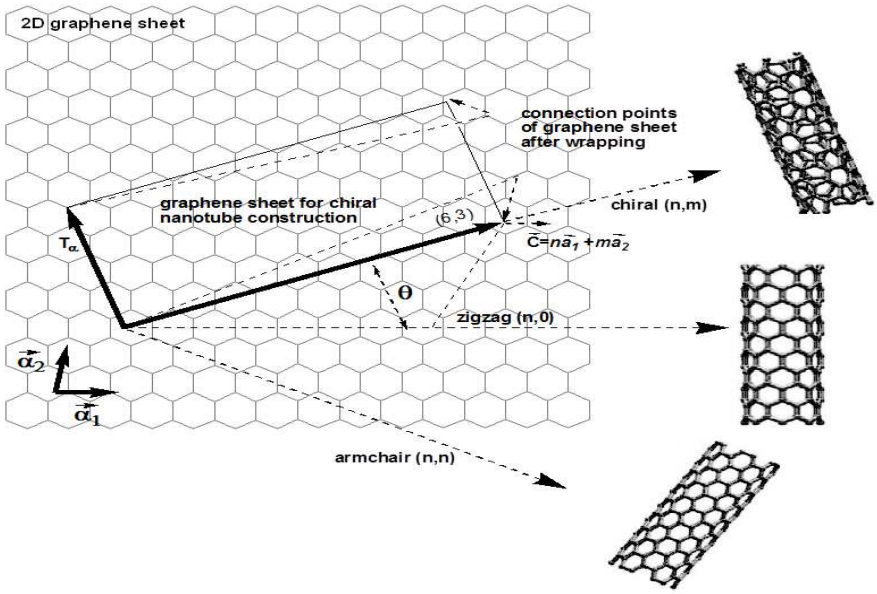

Figure 3. The principle of CNT construction from graphene sheet along the chiral vector $\vec{C}$

The chiral angle θ is defined as the formation of screw angle between zigzag direction and the chiral vector [22]:

$$\theta = \arctan\left(\frac{\sqrt{3}m}{2n+m}\right) \tag{2}$$

In addition, the diameter of the single walled carbon nanotube is defined by:

$$d = \frac{|C|}{\pi} = \frac{\sqrt{3}a\sqrt{m^2+mn+n^2}}{\pi} \tag{3}$$

where C is the circumference and a is the length of carbon-carbon bond in graphene sheet whose value is equal to 1.42 Å [23].
In the next section, it will be discussed which parameters affect the electronic properties of carbon nanotubes.

1.2 Electronic Properties of Carbon Nanotubes

Carbon nanotubes (CNTs) can exhibit metallic or semiconducting behaviour depending on how the graphene sheet is rolled to form the cylinder of the nanotube because this modifies the band diagram of graphene (as explained in section 1.1.2). The study of the electronic features of carbon nanotubes, i.e. either semiconducting or metallic gives the ability to us to control these properties and use them for specific applications. In this section, the band structure of graphene will be explained.

1.2.1 Band Structure of Graphene

The electronic properties of graphene is related to its particular band structure. Figure 4 represents a schematic of a carbon nanotube band structure. Wallace introduced a tight-binding model for electronic band structure of graphene [4, 24]. Based on this model, the conduction (π^*) and valance band (π) of graphene was formulated by considering the low-energy bands of the band structure, which are approximated "as cones with apices at the K-point in the graphene Brillouin zone"[4]. The band structure of carbon nanotube is composed of two large "tent". The conduction band, π* is above and valence band π is behind the K-point respectively [25]. The K-point is at the vertices of hexagon where the conduction band and valence band of graphene touch each other or degenerate [26]. This point is the highest equilibrium occupied state which corresponds to the Fermi energy. The Fermi level, in turn, corresponds to the zero level energy and therefore it coincides with the six points K [27] .

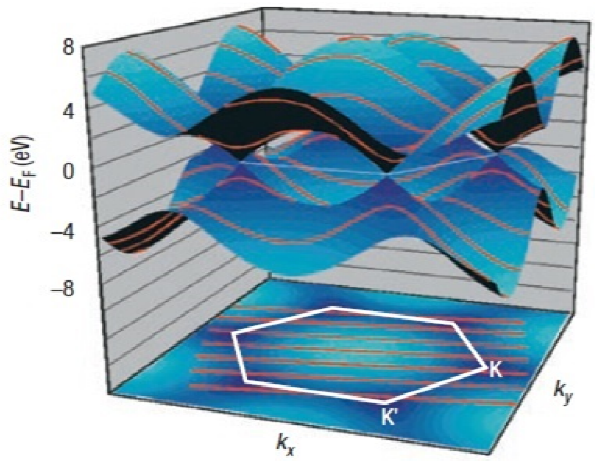

Figure 4. Graphene electronic band structure consists of two bands (Upper and Lower part) that intersect only at a few points (K-point) at the corners of a hexagonal Brillouin zone. Reproduced with permission from Ref. [25]. Copyright 2007 Nature publishing Group.

These **K** points are responsible for the electronic properties of graphene and of its semimetallic behaviour. The degeneracy or touching of the bands at the K point is because of the absence of a bandgap which explains the metallic behaviour (zero-band gap semiconductor) of graphene [16, 25]. In fact, the electronic properties of graphene are related to the energy states around the Fermi level where the electronic states are located on cones whose centres coincide with the **K** points [28] as shown in Figure 4. Around this point, the electron has not the typical parabolic dispersion as in free space or in a material, $\mathbf{E} = \hbar^2\mathbf{k}^2/2\mathbf{m}^*$, ($\hbar$ is the reduced Planck's constant, $\mathbf{k}$ is the wavevector and $\mathbf{m}^*$ is effective mass), but the dispersion becomes $\mathbf{E} = \mathbf{v_F}\hbar\mathbf{k}$, where $\mathbf{v_F}$ is the Fermi velocity of electrons in graphene [29]. This relation is similar to that of mass-less particles like photons, for which $\mathbf{E} = \mathbf{c}\hbar\mathbf{k}$, where c is the light speed [30, 31]. Therefore, in the band π and π^*, near the K points, the electrons and holes in graphene become similar to mass-less quantum particles. In this case "electrons and holes are called Dirac fermions " and K points are often called the Dirac points [26, 31].

1.2.2 Metallic and Semiconducting SWCNTs

SWCNTs can exhibit metallic or semiconducting behaviour depending on the geometric structure of the SWCNT because this modifies the band diagram of graphene as discussed in section 1.2.1. The direction of rolling and the diameter of the nanotube can be obtained from the pair of integers (n, m) which identify the metallic or semiconductor type of tube. This is attributed to the quantum confinement effects when a 2D graphene sheet rolls into the 1D single walled cabon nanotube [4]. To determine the Brillouin zone inherent to the bi-dimensional unit cell of the CNT, defined by the chiral vector C_h pointing along the circumference direction(and the translation vector T shown in Figure 5(a), the corresponding vectors of the reciprocal lattice, C^* and T^*, (parallel to C and T and having a length $\frac{2\pi}{|C|}$ and $\frac{2\pi}{|T|}$) can be constructed [30]. The Brillouin zone of the CNT is given by the rectangle described by C* and T* [30]. When the bi-dimensional unit cell of the CNT is rolled, the electron is bound to moving in a periodic potential, with a period $C = |C|$. This periodicity implies that, due to the stationary condition, the wave associated to the electron, should satisfy the following "quantization condition" [16, 25]

$$C \cdot \mathrm{k} = 2\pi q \quad \text{or equivalently} \quad |C| = \lambda q \tag{4}$$

where q is a not null integer and λ is the De Broglie wavelength associated with the electron.

The quantization condition leads to a discretization of the energy levels along the circumference C, giving rise to a series of lines of quantization corresponding to the allowable values for the pairs (k_x, k_y): the component of k perpendicular to the axis of the CNT, $k_\perp$, can take discrete values (red parallel line), while the component of k parallel to axis of the CNT, $k_{/\!/}$, remains a continuous variable, as shown in Figure 5(b). Therefore, the electrons are free to roam in the direction of the length of the CNT. The quantization condition can be reformulated as $k/C^* = q$. Therefore, to stay in the first Brillouin zone it must be $0 \leq q \leq N$. This means that there are N discrete values of k in the direction of the chiral vector.

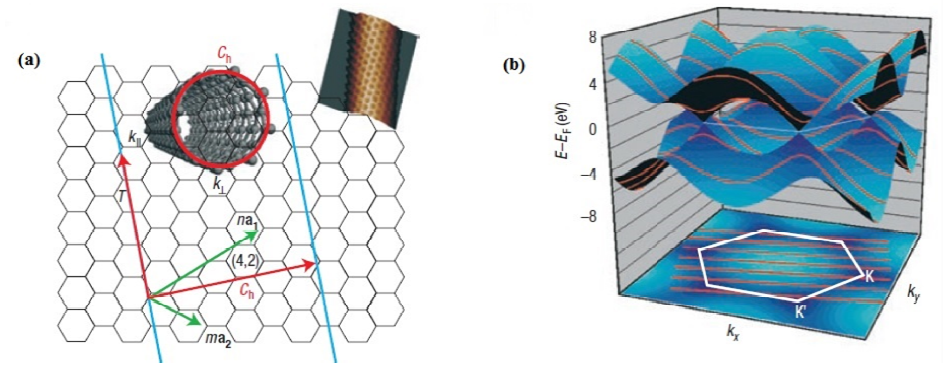

Figure 5. "The structure of graphene and carbon nanotubes". (a) "The carbon atoms in a single sheet of graphene are arranged in a honeycomb lattice". "The insets show the definitions of $k\perp$ and $k||$ (left) and a scanning tunnelling microscope image (right) of a single-walled nanotube". (b), "The band structure (top) and Brillouin zone (bottom) of graphene. The valence band (which is of π-character) and the conduction band (π*-character) touch at six points that lie at the Fermi energy" . Reproduced with permission from Ref. [25]. Copyright 2007 Nature publishing Group.

The planes parallel to the y-axis (energy axis) pass through the quantization lines cutting the dispersion graph of graphene in slices as shown in Figure 5(b) where (E, $k_{/\!/}$) are the 1D sub-bands in the scatter plot of the CNT. In the space of reciprocal lattice, quantization lines are spaced by an amount equal to:

$$\Delta k = \frac{2\pi}{|C|} = \frac{2}{d} \tag{5}$$

depending exclusively on the diameter of the nanotube (d).
As anticipated, depending on the direction in which the graphene sheet is wrapped, it is possible to identify CNTs of zig-zag, armchair or chiral type [20]. The band structure and arrangement of armchair and zigzag nanotubes are shown in Figure 6(a) and 6(b) respectively. In this case, the intersections between the lines of the allowed wave vector k and cones of the dispersion diagram in the *K* points change. For this reason, SWCNTs may have different electrical characteristics [32]. In particular, if the CNT is wrapped around the y-axis ($k_{/\!/}$) the CNT is a zig-zag type and lines of quantized wave vector do not pass through any *K* point and the cut does not intersect the cones apices.

Therefore, in the dispersion diagram of CNT, there will be a gap between the valence and conduction band and CNT will present semiconductor behaviour, Figure 6 (a). Instead, if the CNT is wrapped around the x axis ($k_\perp$) it is an armchair type. In this case, CNT present a metallic behaviour, Figure 6 (b).

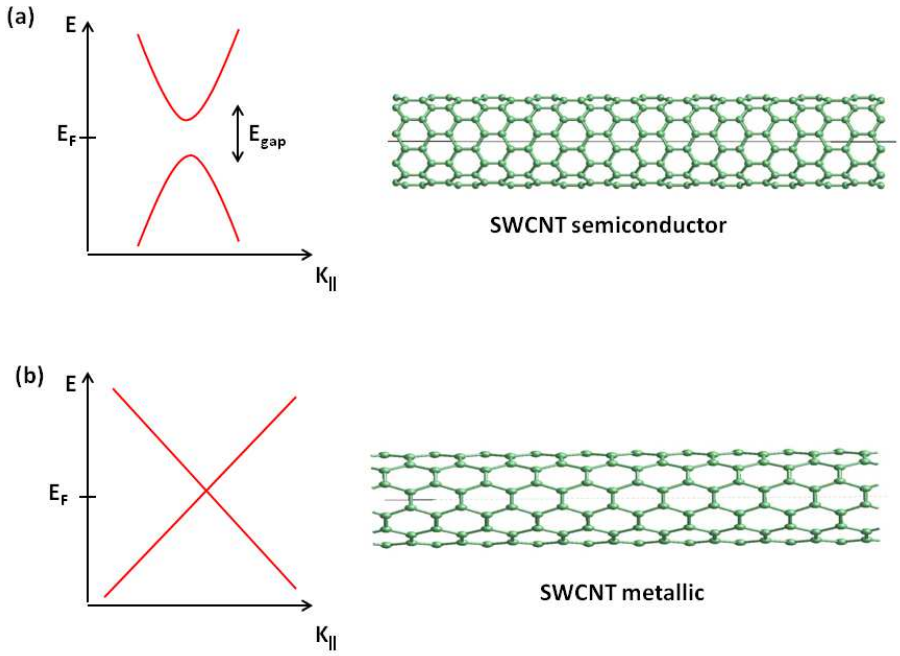

Figure 6. (a) The 1D sub-band nearest to the Fermi level does not intercept the point K1, so a band gap is formed and the CNT shows a semiconductor behaviour (b) The 1D sub-band nearest to the Fermi level passes through the point K_1 and the CNT shows metallic behaviour.

For chiral carbon nanotube with specific (n, m), the nanotube is metallic if n – m = 3i with i is an integer. [16]. All others are semiconductors with a band gap inversely proportional to the diameter of the nanotube [4] Therefore, 1/3 of the carbon nanotubes are predicted to be metallic, and the other 2/3 nanotubes are semiconducting.

As summary, the behaviour of carbon nanotubes depends on their chirality and can be classified into three categories:

a) Zigzag if $n \neq 0\ m = 0$

b) Armchair if $n = m \neq 0$
c) Chiral if $n \neq m \neq 0$

However, not any kind of CNTs is synthesized based on the rolling of graphene sheet. In fact, CNTs are grown with various chemical and physical processes. These various methods lead to carbon nanotubes having different electronic properties, different chirality and different distribution of diameters [33, 34]. Statistical studies show that each batch of carbon nonotubes contains 2/3 semiconducting and 1/3 of metallic type [35] regardless of the specifics how the carbon nanotubes are synthesized. Moreover, increasing the layer thickness of carbon nanotubes elevates the overall conductivity leading to a metallic behaviour.

1.3 Fabrication and Modelling of Devices based on Carbon Nanotubes

In this section, the application of carbon nanotubes, particularly semiconducting single walled carbon nanotubes as an active layer for fabrication field effect transistor, will be discussed. Furthermore the use of this device for chemical/bio sensing will be also briefly explained.

1.3.1 Carbon Nanotube Electronics Device

The invention of the Field Effect Transistor (FET) in 1960 has revolutionized the life style in communication, computing, medical and digital systems. Nowadays, electronic devices are demanded to be smaller and faster. “According to Moore’s law the dimensions of individual devices in an integrated circuit have been decreased by a factor of approximately two every two years”[36, 37]. However, challenges for fabrication of small dimension transistors still remain. Therefore, in order to reduce the dimensions of transistors, while enhancing performance of the devices, another material that has improved properties at molecular scale is needed for replacement of silicon [38]. A great research activity is focused towards substitution of silicon with other materials. Among these materials, carbon nanotubes, due to their exceptional electrical properties such as high mobility at room temperature, high current density, ballistic electron

transport and nano-structure [39, 40] can be an alternative choice. Field effect transistor based on SWCNT has a structure similar to Metal-oxide-semiconductor FET (MOSFET) [41]. The semiconducting SWCNTs are used as active channel material allowing for conductivity modulation. Source (S) and drain (D) electrodes are metallic and gate electrode is formed either as back-gate or top-gate [42], as shown in Figure 7 .

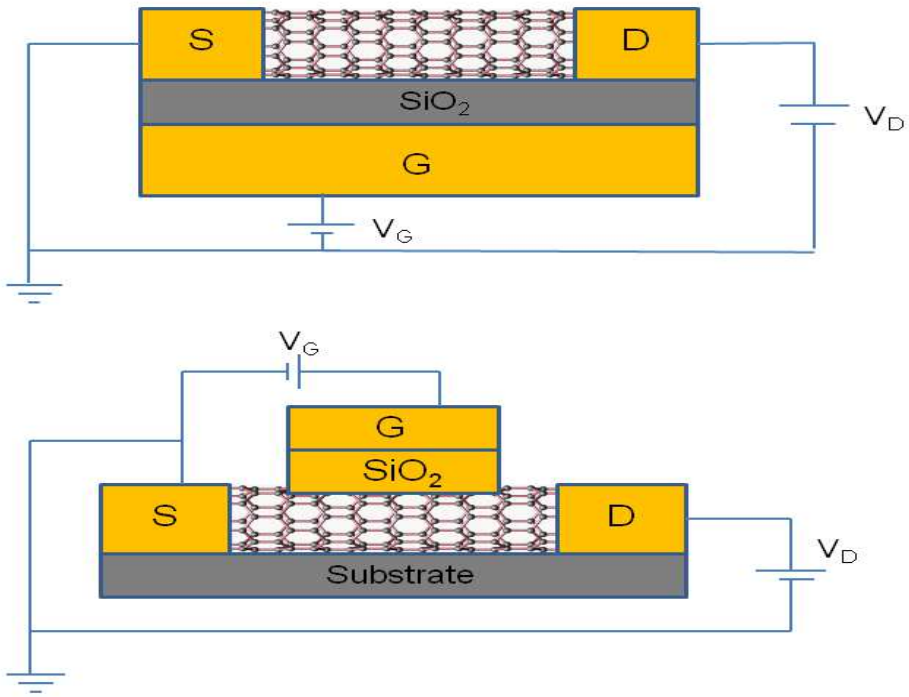

Figure 7. Structures of individual SWNT based field-effect transistors: a back-gate transistor (top) and a top-gate transistor (bottom)

The electric current in SWCNT-FET is based on the fundamental operation principal of FETs : the vertical electric field (gate voltage) is responsible for control of the charge in the channel by inducing charge carriers while the horizontal electric field (drain-source voltage) between the contacts imply the electric force that moves the charge carrier from one contact to the other [16, 43]. Therefore, drain current (I_D) modulated by gate voltage (V_{GS}) is quantitatively explained by

the transconductance (g_m) as fundamental parameter of FET which correlated to the charge carrier mobility [44, 45]:

$$g_m = \frac{\partial I_D}{\partial V_{GS}} \tag{6}$$

Via equation 6 it is possible to determine the charge carrier mobility of a transistor [46]:

$$\mu_{FET} = \frac{L_C}{V_{DS} C_g} \cdot \frac{g_m}{W} \tag{7}$$

where L_C and W are channel length and width respectively, and C_g is capacitance of gate oxide.

Although single walled carbon nanotube thin film transistor (CNT-FET) and MOSFET based silicon have the same structure, the first works in accumulation mode due to the use of intrinsic semiconductor, whereas the latter operates in inversion mode due to the use of doped semiconductor [44].

The individual nanotube transistors show high carrier mobility in the range 3,000 cm^2/Vs [47, 48]. However, the assembly method of individual SWCNTs is highly challenging for technologically applicable solutions for large-scale applications. So, the complex process for making individual SWCNT-FET prevents the commercialization of this type of device [49]. Therefore, thin film based on semiconducting SWCNTs represents a promising track to scalable device manufacturing since this approach avoids the cumbersome procedure for precise control over the position of individual carbon nanotube. SWCNTs -TFT structure based on the spatial arrangement of SWCNTs in the channel of TFTs are categorized as aligned [47, 50] and random network [51-54] as illustrated in Figure 8.

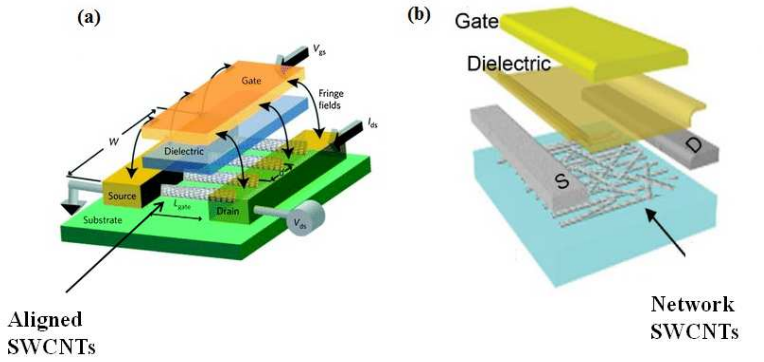

Figure 8. Schematic illustration of a top-gate SWCNT-TFT (a) aligned SWCNTs. Reproduced with permission from Ref. [55]. Reproduced with permission from Ref. [55]Copyright 2009 Nature Publishing Group. (b) random network SWCNTs [56]. Reproduced with permission from Ref [56]. Copyright 2008, Tsinghua University Press and Springer-Verlag Berlin Heidelberg.

Figure 8 shows a top-gate SWCNTs-TFT either with aligned or random network of SWCNTs. The structure and electronic characteristics of the bottom-gate SWCNTs TFT, which has been used in our experiments, will be shown in chapter 3.

Fabrication of transistors based on randomized SWCNTs thin film, compared to that based on single CNT, has a better reproducibility over large area [57].

One of the most important parameters for fabrication of SWCNTs-TFT is how much percentage of semiconducting SWCNTs are used in the active layer in the channel. In fact, synthesized SWCNTs are generally a mixture of semiconducting and metallic nanotubes with variable distribution of chiralities and diameters, resulting in heterogeneous electrical properties [58-62]. If the density of metallic nanotubes is higher than the percolation threshold, a shorted TFT is obtained.

Figure 9 shows a plot of the gate voltage dependence of the conductance of either metallic or semiconducting nanotube device at room temperature.

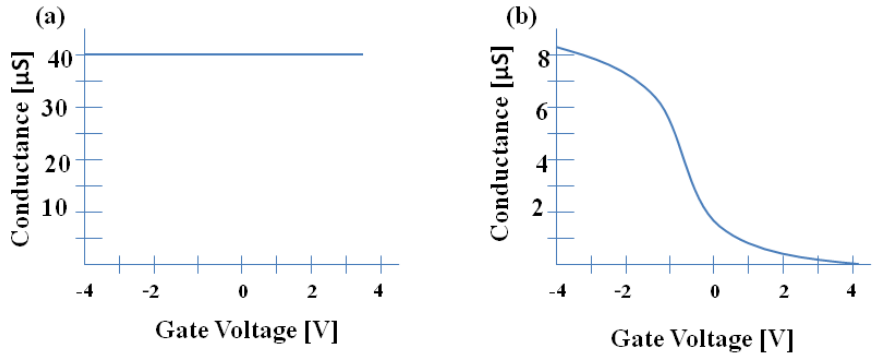

Figure 9. Examples of the gate-voltage dependence of the conductance through a SWCNT at room temperature for (a) a metallic and (b) a semiconducting nanotube

Figure 9(a) shows the conductance of metallic carbon nanotube at a constant bias-voltage along it, while the gate voltage is changing. The current is independent of gate voltage [4]. On the other hand, Figure 9(b) shows the same plot for a device made from a semiconducting carbon nanotube. This device is able to be turned on and off by applying negative and positive gate voltage respectively. Moreover, the conductance changes by order of magnitude between on and off state. This is attributed to the utilization of a sufficiently high percentage of semiconducting carbon nanotubes. In fact, when there is no gate voltage, just metallic SWCNTs contribute to the current of transistor (I_{off}) while when voltage gate is applied, the transistor turns on and a combination of semiconducting and metallic of SWCNTs are responsible for the current (I_{on}). Hence, the ratio of on-current to off-current related to the ratio of semiconductingvs. metallic SWCNTs .

In order to profitably employ semiconducting SWCNTs, post-synthesis fabrication furnishes a reliable alternative for separating the semiconducting SWCNTs from the metallic ones. This process will be discussed in chapter 2.

A next step for fabrication of SWCNTs-TFT is the deposition process. Researchers have developed various techniques to deposit carbon nanotube thin films on substrates. These various techniques and their detailed procedures for deposition of CNT thin film will be discussed in chapter 2, while our technique with its advantages will be discussed in chapter 3.

1.3.2 Carbon Nanotube Bio/chemical sensing

Since the discovery of carbon nanotubes, great efforts have been done to explore this material for bio/chemical sensing due to the unique electrical characteristics and bio/chemical compatibility [63-65]. The response of SWCNT to biomolecules is linked to the nano-structure of this material comparable to the dimension of bio-molecules such as DNA or proteins [66, 67]. Moreover, the shape of SWCNT shows capillarity properties. The high aspect ratio (i.e. length to diameter ratio) makes them one of the ideal material for the adsorption of gases and chemical components [68]. In addition high surface area (~ 1300 m^2/g) [69] of SWCNT cause more bio/chemical molecules to interact with the carbon nanotube surface which leads to a high sensitivity [70].

In order to use of SWCNT as a biosensor, it is needed to integrate them with electronic devices such as transistors or chemo-resistors as a transducer [48, 63]. The schematic of a biosensor based on SWCNT-FET for DNA detection is shown in Figure 10. The advantages of these sensors, compared to the traditional ones, are the possibility of obtaining selective systems, reversible and able to operate at room temperature with very quick response times.

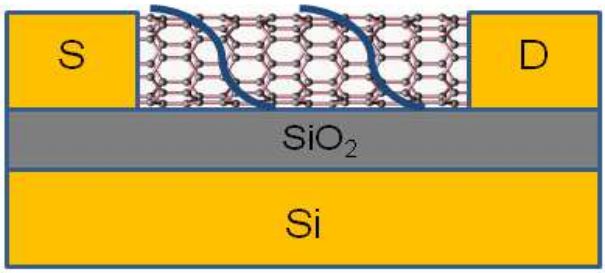

Figure 10. Schematic of DNA-functionalized carbon nanotube biosensor

The bio-sensing function is based on the conductance variation when bio-molecule interacts with the surface of SWCNT due to change of electrical properties of the device [71]. Various biomolecules, for instance DNAs and proteins, can interact with the surface of SWCNTs, due to hydrophobic, $\pi - \pi$ stacking interactions [60, 72], and also amino-affinity of SWCNTs to change the conductance of SWCNT thin films [73]. The mechanism for detection of specific

protein, immobilization procedure and sensitivity of thin film SWCNTs based label-free bio-sensor will be explained in detail in chapter 5.

1.3.3 Modelling of Carbon Nanotube Device

In order to improve the SWCNTs-TFTs performance, the modelling of the charge transport on the SWCNTs network inside the channel of TFT devices is an important issue to investigate. This modelling shows the relation between the physical characteristics of SWCNTs and the geometrical structure of TFTs. Several authors have studied this problem by considering a physical arrangement of the SWCNT network in a 2 dimensional (2D) model [74, 75]. Figure 11 shows the 2D simulation of nanotube network inside the channel of TFT structure.

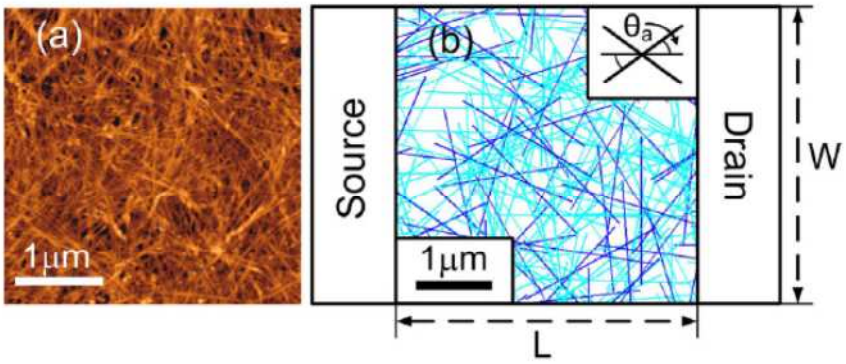

Figure 11. (a) "Atomic force microscope (AFM) image of a CNT film where nanotubes are randomly distributed". (b) "A 2D nanotube network generated using Monte Carlo simulations for a device. Semiconducting and metallic nanotubes are shown in light and dark color (cyan and blue color), respectively. The inset illustrates the alignment angle θ_a , which defines the angle range within which nanotubes can be generated to form partially aligned CNT films in simulations". Reprinted (Fig.1) from Ref. [75] .Copyright (2008) by the American Physical Society Publishing Group.

However, the use of a 2D model presents some limitations due to the impossibility to investigate change in the diameter of carbon nanotubes (represented as sticker rather than a cylinder). Due to the role assumed by the geometric characteristics of the SWCNT and TFT structure that affect on electrical response of a device, a 3D study of the problem by numerical simulations has been developed and it will

be described in chapter 4. In addition, the results obtained by simulations are compared with experimental ones to understand which parameters control the performance of device and to investigate the correlation between the percolation condition and the density of CNT network.

Chapter 2

State-of-the-art

In order to optimize the performance of electronic devices based on carbon nanotubes, researchers have investigated various ways to effectively manipulate them. There are two fundamental protocols for the assembly of thin film carbon nanotubes on substrate: 1) direct growth based on chemical vapour deposition (CVD) [76, 77]; 2) post-process deposition technique [54, 78].
This chapter is devoted to the illustration of both methods and reports the advantages of the solution deposition compared to the CVD technique. The solution deposition process not only permits the fabrication process of electronic devices at room temperature but also allows the control of electronic characteristics of either semiconducting or metallic SWCNTs. This technique is compatible for all patterning methods and it is also suitable for all kind of substrate and pre-existing circuit structures. Furthermore, various techniques for solution process deposition will be explained.

2.1 Synthesis of Single Walled Carbon Nanotubes by Chemical Vapor Deposition

One of the most important techniques for the synthesis of carbon nanotubes is chemical vapor deposition (CVD). This method is based on directly growing of CNTs on substrate. The procedure is as follows: the solid substrate is placed in a high temperature furnace (i.e. 600 – 1000 °C) [79-81] and transition metallic catalysts such as Fe, Co, Ni [81] in nano-scale size are inserted in the furnace with ethanol or ethylene as a feedstock for converting the carbon source to form a new nucleation site for CNT growth [82]. Carbon sources, hydrocarbons [83] or carbon monoxide at high temperature are

decomposed and absorbed on catalysts [84] and afterward carbon nanotubes grow on the substrate. A scheme of the process is shown in Figure 12.

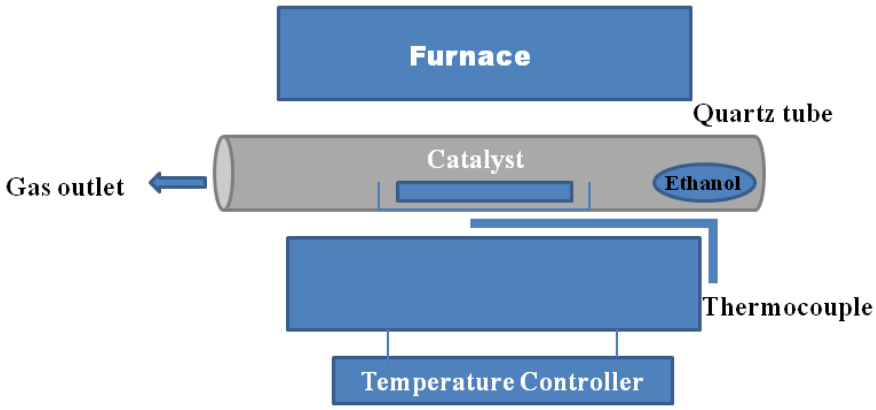

Figure 12. Schematic of CVD for growing CNT

The advantage of this method, compared to other methods for growing CNTs, is that by adjusting the size of catalyst and varying the temperature it is possible to control the diameter, chirality and average length of CNTs [81, 82]. However, with this method a mixture of semiconducting and metallic nanotubes is produced. Although some progress has been made to control the properties of SWCNTs during growth, none of these methods produce homogeneous electrical properties of SWCNTs batches [85]. Therefore, in order to overcome this problem, it is required to develop other methods to select features of CNTs with optimized properties for specific application [86, 87].

2.2 Single Walled Carbon Nanotubes Solution and Preparation

As explained in section 2.1, the growth of SWCNTs on substrates with conventional CVD has to be performed in a high temperature environment, i.e. 900 °C. As a consequence, there is a limited to choice of substrates and pre-existing circuit structures [88, 89]. Moreover, electrical characteristics of grown SWCNTs are difficult to control. In fact, the synthesized SWCNTs are generally a mixture of

semiconducting nanotubes and metallic ones with variable distribution of chiralities and diameters, resulting in heterogeneous electrical properties [48, 58, 59, 61]. Therefore, in order to employ SWCNTs, post-synthesis deposition furnishes a reliable alternative by overcoming the high temperature problem and the expensive procedure for growing semiconducting SWCNTs. This method enables to separate semiconductive from metallic SWCNTs and it is useful for the optimal performance of devices. In order to deposit SWCNTs from solution, it is required to disperse them in an aqueous surfactant [59, 85, 90] or organic solvent [91-94] because of the inherent insolubility of them in aqueous solution. There are two main methods to disperse SWCNTs in solution: 1) chemical functionalization [95, 96] or covalent-functionalization; 2) physical interaction or non-covalent functionalization [97, 98] . In both methods, the batch of carbon nanotubes containing of mixture of metallic and semiconducting entities (also with various length and diameters) needs to be dissolved in specific solution. In the covalent process, SWCNTs are treated with strong acids and oxidants and a carboxylic acid (COOH) functionalization is produced [99]. However, the harsh conditions, alter the electronic properties of the SWCNTs [96, 100]. An alternative approach to disperse SWCNTs is the non-covalent functionalization or physical interaction. This technique disperses SWCNTs in aqueous solution preserving the electrical properties of SWCNTs.

Generally, grown carbon nanotubes are in bundle form due to the strong Van der Waals interaction [101] and hence it is needed to de-bundle and suspend them in aqueous solution. Moreover, carbon nanotubes are a non-polar material and have a hydrophobic surface [6] and they are not dissolvable in water. Hence, in order to increase their solubility it is needed to attach amphiphilic surfactants to their surface [102]. The amphiphilic surfactants have a hydrophobic tail and hydrophilic head [6]. The hydrophobic tail interacts with hydrophobic surface of SWCNT via hydrophobic/hydrophobic interaction, while hydrophilic head facilitates the dispersion in aqueous solution [97]. The wrapping of the surfactants around the SWCNTs is shown in Figure 13. Then, by the help of sonication the Van der Waals forces between tubes are overcome and the conversion of the bundle to the individual SWCNTs takes place [102, 103]. The surfactants, in fact, deposit on the surface of SWCNTs and being charged, introduce

electrostatic repulsion and stabilize the isolated single CNTs in solution [96].

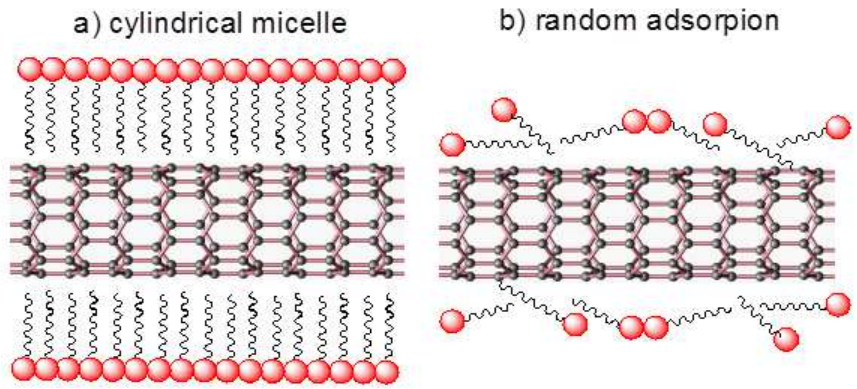

Figure 13. Schematic illustration of various surfactant assembly structures on a SWCNT, including (a) cylindrical micelles, side and cross-section views, (b) hemimicelle, and (c) random adsorption

After that, the centrifugation of the solution separates the SWCNTs from amorphous carbon and remove large bundle that still remain in solution [85].
surfactants able to disperse Successfully SWCNTs in aqueous solutions are: sodium dodecyl sulfate (SDS)[104, 105], sodium dodecylbenzenesulfonate (SDBS) [106, 107], and Triton X [108, 109].
Recently, by using density gradient ultracentrifugation (DGU) the separation of semiconducting SWCNTs from metallic ones as reported in Figure 14 [85], has been achieved. In this condition, low density smaller-diameter semiconducting SWCNTs are found on the top layer of the vial. On the other hand, high density metallic SWCNTs settle at the bottom of the vial. As it can be seen from Figure 14, observed different bands verify the sorting of SWCNTs based on their diameter as identified by UV-Vis spectroscopy [85].

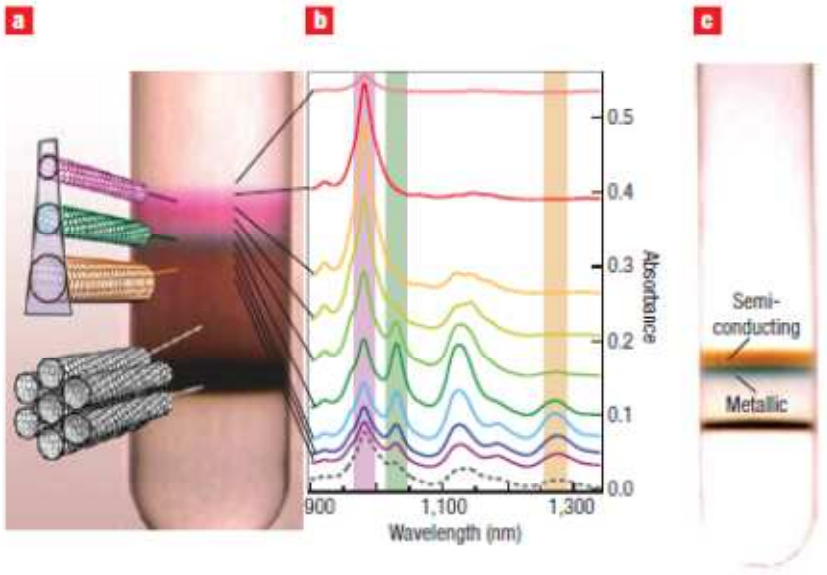

Figure 14. Sorting SWNTs using density gradient ultracentrifugation (DGU). a, Small-diameter (0.7–1.1 nm) SWNTs encapsulated with sodium cholate are sorted by diameter following DGU. b, Optical absorbance spectra for different fractions, further confirm sorting by diameter. c, Large-diameter SWNTs are sorted according to electronic type following DGU. Reproduced with permission from Ref. [85]. Copyright 2008 Nature Publishing Group

2.3 Deposition Methods for SWCNTs Solution

The assembly of SWCNTs from solution provides a strategy for construction of a thin film on a substrate that is technologically applicable for large areas and gives the possibility for fabrication of electronic devices at room temperature. Various methods for deposition SWCNTs in solution for assembly thin film have been demonstrated such as spray coating [88], dip coating [65], spin coating [90], dielectrophoresis deposition [89], and electrophoretic deposition [110]. This section will report these techniques.

2.3.1 Spray Coating

One of the techniques to form SWCNTs thin film from solution is spray-coating. The schematic of a spray coating system is shown in Figure 15. The system is based on a pistol which is composed of three main parts for control the process and a hot plate for acceleration drying process [111]. The mechanism is as follows: 1) Vessel is used for inserting SWCNTs solution, 2) atomizer is utilized to form an aerosol from the solution 3) atomizer control the injection of solution for transporting the droplet from nozzle to destination substrate by controlling gas flux and position of pistol.

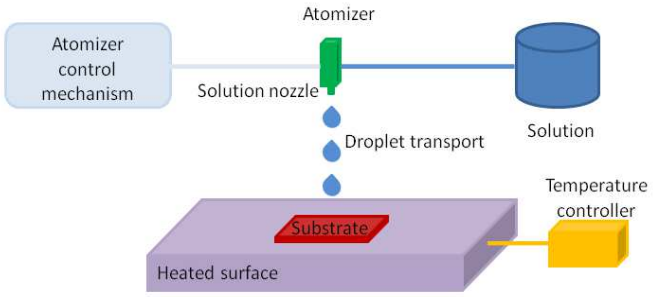

Figure 15. Schematic of spray-coating

M. Jeong *et al.* utilized spray-coating deposition to form SWCNTs thin film from solution on substrate for transistor fabrication [112]. In order to enhance the deposition, they used 3-aminopropyltriethoxysilane (APTES) for silanization of the substrate and sprayed the solution on the top of the hot plate at 100 °C in order to accelerate the evaporation of the solvent. Although this method is simple and allows the control of the thickness of the thin film by repeating the process, however, due to the relatively high temperature needed for coating, it is not suitable for thermally sensitive substrates, particularly for flexible substrates..

2.3.2 Dip Coating

Another method to create a thin film of SWCNTs from solution is dip-coating. In this method, a substrate is immersed and pulled up in bath

solution with specific speed and continuously depending on the desired thickness of thin film [113, 114] . A schematic of the process is shown in Figure 16.

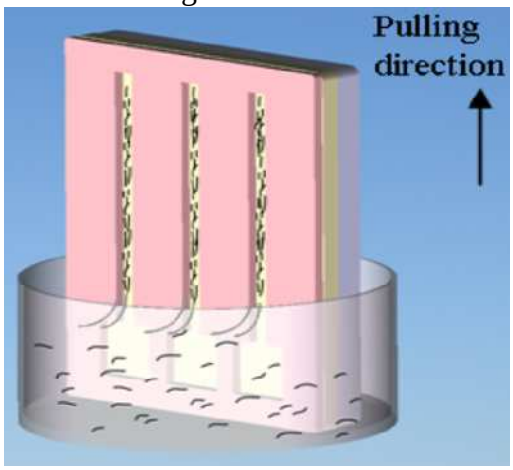

Figure 16. Schematic of deposition dip-coating. Reproduced with permission from Ref. [114]. Copyright 2009 IOP Publishing Group

X. Xiong *et al.* applied dip-coating method with photolithography for selective assembly of SWCNTs network on the polymer substrate (parylen-C) [114]. This process is based on a difference in surface energy. The micro-trenches which were patterned by using optical lithography have a hydrophobic surface and SWCNTs were not absorbed on its surface. Therefore, it is needed to modify the surface to become hydrophilic. In this case, the surface become hydrophilic by utilizing O_2 plasma treatment and thus SWCNTs were attracted on the modified hydrophilic surface. This method allows the SWCNTs selectivity deposited on hydrophilic surface on the micro-trenches by dip-coating method. This method is quite simple and cost-effective. However, this process not only need a special instrument to control the deposition process and is difficult to handle process, but also the surfactant-wrapped SWCNTs can degrade the electronic properties of device.

2.3.3 Spin Coating

Spin-coating is a process for assembly of thin films on a flat substrate. A specific amount of solution is dispensed on the substrate while rotating at specific speed. Therefore, the solution spreads on the

substrate by shear forces [100, 115]. In this manner, the solvent evaporates and the SWCNTs remain on the substrate. A schematic of spin-coating is shown in Figure 17.

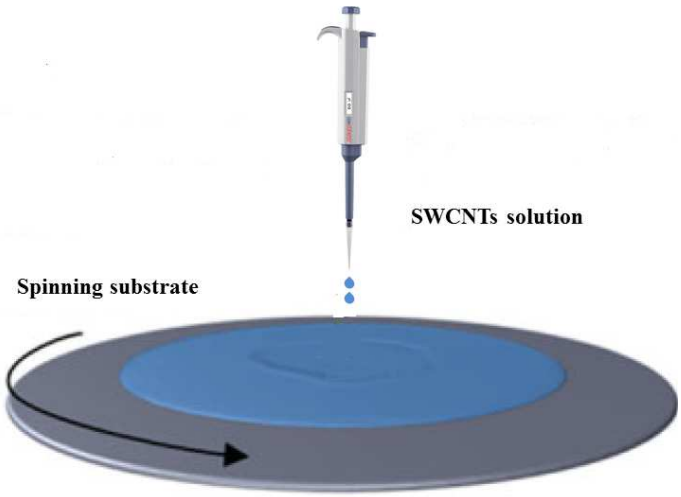

Figure 17. Spin-coating process. Used in part of this figure is Reprinted with permission from Ref. [116]. Copyright 2004 American Chemical Society.

LeMieux *et al.* have used spin-coating for assembly of thin films of SWCNTs in the fabrication of transistor based on the self sorted technique [117]. In order to overcome hydrophobic surface of SWCNTs for enhancing attachment on the substrate, they used two types of silanes with amino and phenyl groups for the substrate functionalization. The amino-terminated surface causes more semiconducting SWCNTs to be attracted on it while phenyl-terminated surface leads to the attachment of more metallic ones. The same authors showed later that, by controlling the volume of SWCNTs solution and rotational speed of the spin coating device, the SWCNTs can be aligned in the channel of TFT structures. [118]. However, the spin coating approach for the deposition of SWCNTs is suitable for device arrangement compatible with the dimension of the rotating equipment and therefore limited to small scale arrays.

2.3.4 Dielectrophoresis Deposition

Another method for assembling SWCNTs thin films is dielectrophoresis. In this method, carbon nanotubes become polarized

under an anisotropic electric field which align them between two electrodes [119-121]. The schematic for dielectrophoresis is shown in Figure 18. By applying an alternating electric field with specific frequency and voltage allows to align SWCNTs by inducing a dipole on the SWCNT particles in the solution. [122, 123].

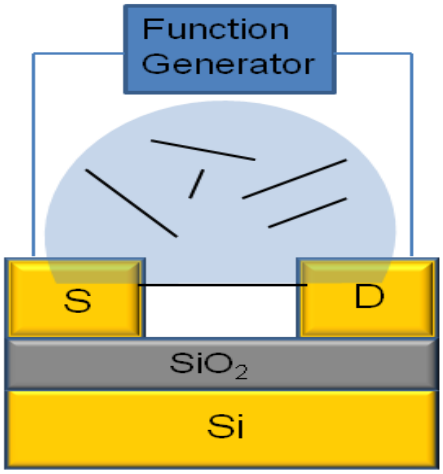

Figure 18. Schematic arrangement for dielectrophoresis-based alignment of CNTs

There are various parameters affecting this process including strength of electric field, electric permittivity of solution and the properties of SWCNTs particles [120]. J. Li *et al.* have fabricated field effect transistors based on this method and have controlled the number of carbon nanotubes on the basis of concentration of SWCNTs in solution and deposition time. Although dielectrophoresis approach leads to align the carbon nanotubes in channel (between the two electrodes), it acts more effectively on the metallic nanotubes than on semiconducting ones.

2.3.5 Electrophoretic Deposition

Electrophoresis is another kind of deposition of SWCNTs solution on the desired substrate. The procedure is as follows: the SWCNTs solution is placed between two electrodes subjected to an electric

field. The SWCNT particles become polarized under the non-uniform electric field and are attracted towards the electrodes. Accumulated SWCNTs on the electrode are collected from the electrode and used for formation of a thin film [82]. The schematic of the electrophoresis process is represented in Figure 19.

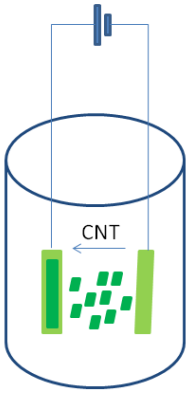

Figure 19. Schematic of electrophoresis deposition

Lima et al. formed thin film carbon nanotubes on a non-conductive substrate for making a transparent conductive electrode [110]. Although this method is simple and quick, it is not technologically applicable for large areas of deposition and it is not able to remove the surfactant from SWCNTs.

Chapter 3
Experimental Process for Fabrication of SWCNTs-TFT

In this chapter the fabrication of thin film transistors (TFTs) based on high purity semiconducting SWCNTs will be described. In the first part, the procedures for dispersing SWCNTs in the surfactant solution will be explained. Afterwards, our effective method, which is a combination of substrate silanization and vacuum filtration method, will be illustrated. Then, the electrical characterization of SWCNTs-TFTs will be presented. Moreover, the advantages of this technique will be discussed.
The schematic of back-gate SWCNTs-TFT is shown in Figure 20.

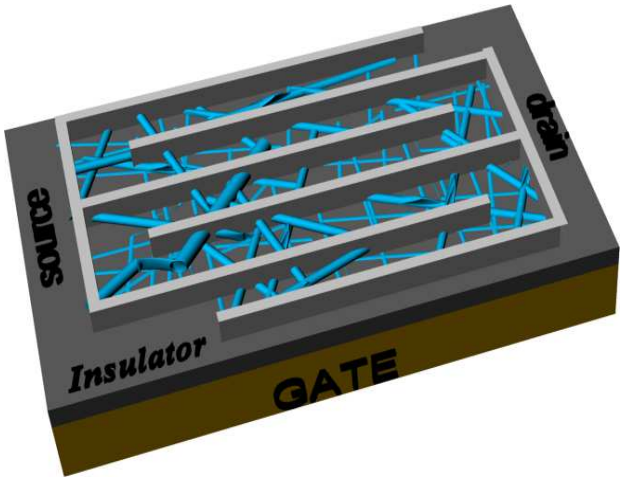

Figure 20. Schematic of SWCNTs-TFT

All the SWCNTs-TFT structures were fabricated and measured at room temperature. The electrode configuration, explained in subsection 3.1.1 followed by a deposition procedure reported in subsection 3.1.2 and 3.1.3, is chosen in order to create the active layer of the structure.

3.1 Dispersion Process of Semiconducting SWCNTs on Aqueous Solution

The 90% semiconducting SWCNTs powder synthesized by CoMoCAT®-CVD method is obtained from sigma-Aldrich Co. (SWeNT® SG-65) [124]. The average diameter of SWCNTs in the powder form is between 0.7-0.9 nm with chirality (6,5). The powder was dispersed in surfactant based aqueous solution. The surfactant was sodium dodecyl benzene sulphonate (SDBS, chemical formula $C_{12}H_{25}C_6H_4SO_3Na$). This ionic surfactant was chosen in order to improve the dispersion of SWCNTs in the aqueous solution [125]. The schematic of the interaction between SDBS and SWCNTs surface is shown in Figure 21.

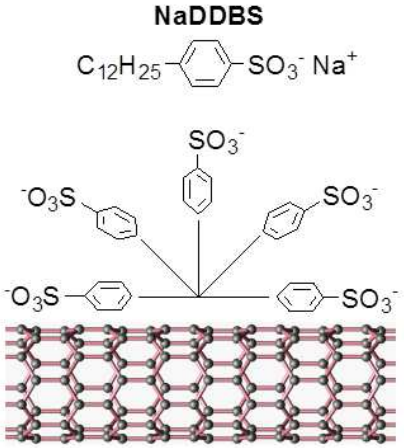

Figure 21. Schematic representation of SDBS and its interaction with SWCNT surface

The procedure for dispersing of SWCNTs in aqueous solution is as follows: 0.05 mg of SWCNTs were added to 1 wt% of SDBS in aqueous solution (deionized water, 10 mL). The SWCNTs powder sedimented in the bottom of vial. In order to disperse them well, i.e. to overcome Van der Waals forces for converting bundle form to individual separated CNTs , the vial was sonicated for 3 hours in ultrasonic bath. In order to prevent the solution from over-heating, ice

was added in the sonicator bath. After that, the suspension was further dispersed in a homogenizer for 15 minutes and then the vial was shaked for 2 minutes. Figure 22(a) shows the dispersion of SWCNTs in SDBS based aqueous solution after sonication. Then, the suspension was centrifuged at 12.000 rpm for 30 minutes. The supernatant consists of individual CNTs, while at the bottom of the vial there were mainly bundle forms of SWCNTs. For this reason, after centrifugation, the supernatant of the vial (almost 50% of top part of the vial) was carefully transferred to a new vial. The remaining part of the solution was sonicated again for 1 hour in ultrasonic bath and then centrifuged. The supernatant of SWCNTs solution after centrifugation is shown in Figure 22(b).

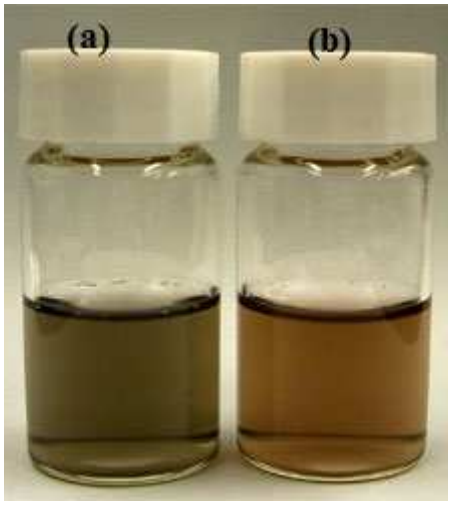

Figure 22. SWCNTs in SDBS solution (a) after sonication and before centrifugation; (b) after centrifugation.

The dispersed SWCNTs solution (top part of the vial after centrifugation) was subjected to UV-Visible spectroscopy and comparedto provided UV-Vis data. The UV-Vis spectroscopy of 90% semiconducting SWCNTs, SG65, and our result of UV-Vis spectroscopy is shown in Figures 23 and 24, respectively.

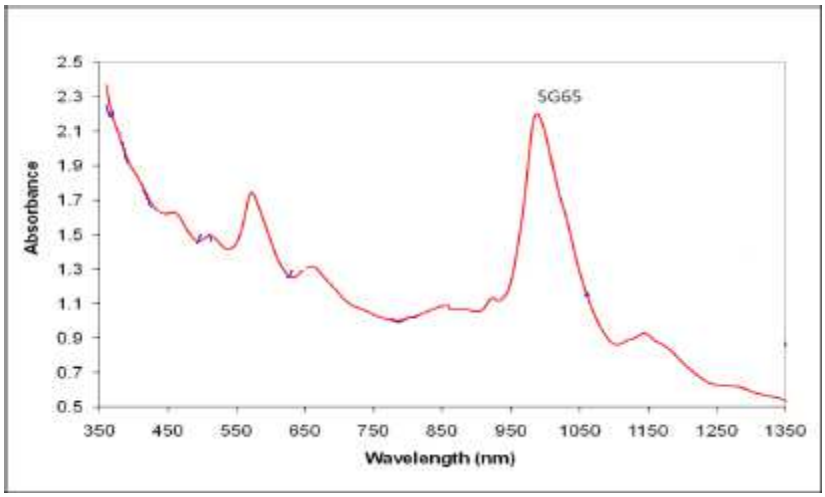

Figure 23. UV-Vis spectroscopy of SG65 (red-line) based on data sheet [124]

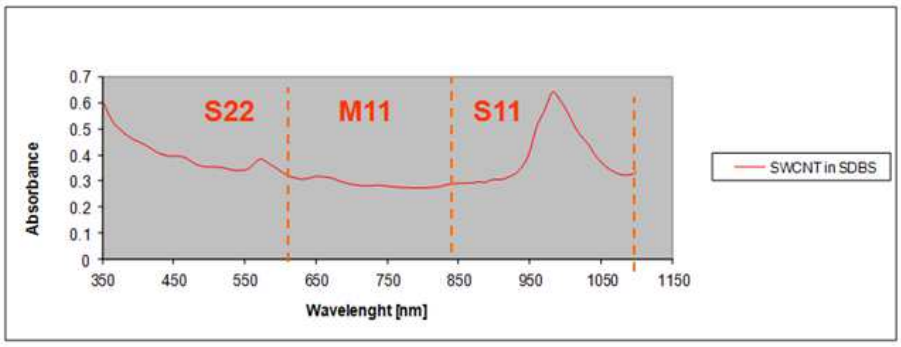

Figure 24. UV-Vis spectroscopy SWCNTs in SDBS aqueous solution.

Peaks from 850 nm to 1100 nm and 450 nm to 600 nm wavelength are conform to first and second semiconducting transition [126], named S_{11} and S_{22}, respectively. Peaks in the range between 600-850 nm are corresponding to the first metallic transition (M_{11}) [116, 127]. The result from Figure 24 shows that SWCNTs powder dissolved successfully in SDBS aqueous solution.

3.1.1 Experimental Process for Fabrication Drain-Source Electrode in the form of Interdigitated Electrode

n-type silicon wafers with a 100 nm thermally oxidized layer SiO_2 were chosen as substrate. First, the surface of the substrate was cleaned to eliminate the inorganic and organic contamination of surface. The procedure is as follows: immersing the diced wafer in acetone followed by ultrasonic bath to remove inorganic contaminations and then cleaning by piranha method which is a mix of H_2O_2 and H_2SO_4 to remove organic contamination and to introduce OH-groups to improve the wetting properties. Second step, the AZ1512 photo-resist was deposited on the surface with spin coating to form a uniform ~1 µm thin film of resist on the surface. Third step, the wafer is exposed to ultraviolet light (wavelength, $\lambda = 0.2\ to\ 0.4\ \mu m$) through a mask containing the desired pattern.. By using an optical lithography system and alignment process, the desired pattern is defined on the substrate. Here we have chosen the mask named mask-Ø11 which includes the interdigitated electrode (IDE) with various channel lengths and widths to form drain and source electrodes of a thin film transistor (TFT). The channel length L_C and width W vary in a 2-dimensional sample space $S = (L_C \otimes W) \in \Re^2$. Each point in this domain refers to a particular sample. The results concerning five samples of SWCNTs-TFTs will be discussed later. Fourth step, the sample is subjected to a post-bake process and it is heated up on a hot plate at 100 °C to eliminate possible traces of the solvent. Thereafter, the photo-resist is developed by 726-MIF developer and the irradiated area was washed away by DI-water and dried with blowing nitrogen. Then the substrates with defined structures were put into a conventional e-beam evaporator (base pressure ca. $1x10^{-5}\ Pa$) to coat titanium with a thickness of 3 nm for good adhesion between gold and the substrate and later the gold with 25 nm thickness. The resist was deposited and then removed by a lift-off process. The schematic of photolithography and metallization steps is shown in Figure 25.

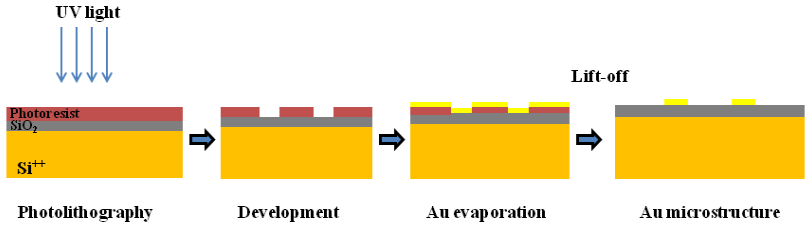

Figure 25. Schematic process for photolithography and metallization

Five samples were considered according to the following parameter S= $\{L_C\ [\mu m], W\ [mm]\} \in \{(2,20),(4,60),\ (8,30),\ (20,8),(50,20)\}$.

3.1.2 Silanization of Substrate

Prior to the deposition of SWCNTs solution on the substrate, the SiO_2 layer was silanized by 3-aminopropyl triethoxy silane (APTES) in order to create amine terminated self assembled monolayers (SAM). The presence of amine group or positive charge in the SAM facilitates the selective absorption of the semiconducting carbon nanotubes network [53, 117, 128]. The schematic illustration of the wafer silanization is shown in Figure 26.

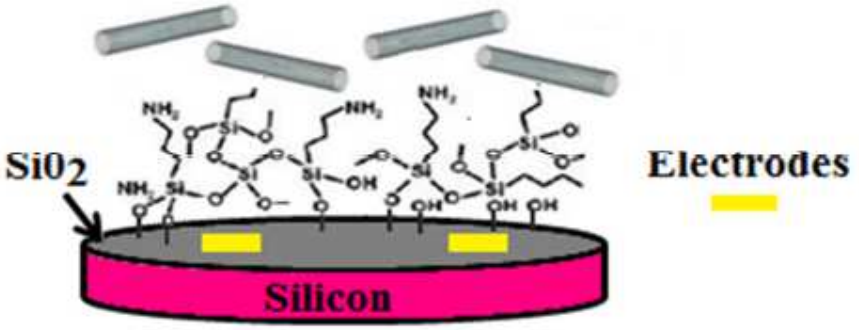

Figure 26. Schematic of silanization with APTES on the substrate.

In order to obtain this SAM layer, substrates were first processed by plasma treatment for 5 minutes, thus allowing the formation of hydrophilic surface. Plasma-treated wafers were soaked in a 1% APTES solution in 2-isopropanol alcohol (IPA) for 15 minutes,

afterwards washed copiously with IPA and dried completely by a nitrogen gun to obtain a homogenous surface

3.1.3 Vacuum Filtration Deposition

The thin film was made by dispersing semiconducting SWCNTs with an effective-deposition technique at room temperature that combines vacuum filtration and silanization of substrate. After APTES functionalization of substrate, the SWCNTs solution was deposited via vacuum filtration technique.
The procedure consists of five steps as reported in Figure 27. A mixed cellulose ester membrane, i.e. filter in Figure 27 (diameter= 47 mm with pore size 0.22 μm), was placed on vacuum filtration apparatus and 1 ml of 90% semiconducting SWCNTs solution with concentration 0.05mg/ml was then quickly vacuum filtered. As the solvent passes through the filter, the carbon nanotubes were entangled with the surface of the filter, creating a carbon nanotubes network with wrapped surfactant, i.e. filter/SWCNTs/surfactant in Figure 27 (Vacuum filtration, step 1). Afterwards, by rinsing off the filter covered with SWCNTs/surfactant with 100 ml deionized water (DI-water in Figure 27), it is possible to dissociate the surfactant from SWCNTs network (Surfactant dissociation, step 2). Then the filter covered by the SWCNTs network was placed onto the silanized substrate, i.e. the pink rectangle of Figure 27 (Transfer to destination, step 3). A gentle press on the top was applied for one hour by using a glass sheet in order to obtain a good SWCNTs distribution with applied force (Press, step 4). Finally the SWCNTs network was transferred by dissolving the filter on the substrate surface in an acetone and methanol bath until the filter disappeared from the surface (Filter dissolution, step 5) and a thin film of SWCNTs network remained on the surface.

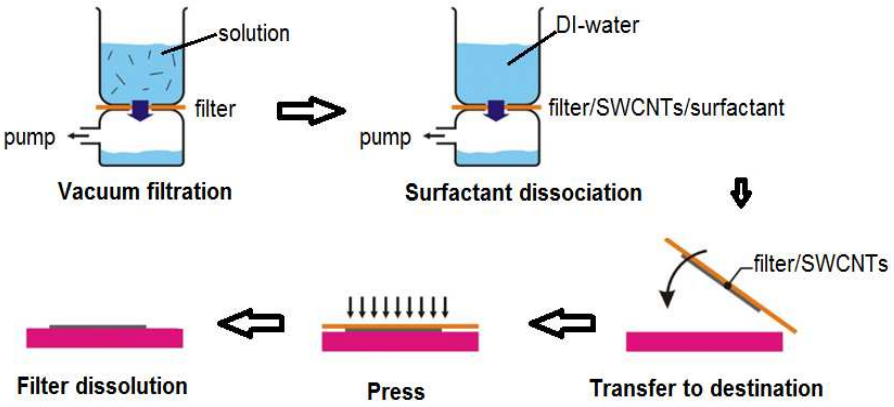

Figure 27. Schematic of vacuum filtration steps

Vacuum filtration method has been found to be an effective approach for a reproducible process for fabrication of SWCNTs films with specific film density [129, 130]. The density of carbon nanotubes network can be specified by controlling the volume of CNT solution used to be filtered through the membrane. In addition, this method has an advantage that the speed of vacuum filtration prevent the tubes from flocculation [131]. Moreover, the dissociation of surfactant from SWCNTs allows preserving the electrical characterization of SWCNTs which enhances the yield of the devices. This deposition process has advantages such as to be inexpensive, scalable to large areas and to be allow the transfer of the thin film to all kind of substrates and pre-structured circuits by membrane dissolution.

3.1.4 Electrical Characterization of 90% Semiconducting SWCNTs-TFT

SWCNTs-TFTs in a back gate and bottom contact configuration with different channel lengths and widths (L_C, W) in the sample space S were taken into account. In particular, 5 samples are considered according to the following parameter space S= (L_C [µm], W [mm]) ∈ {(2,20), (4,60), (8,30), (20,8), (50,20)}. The network of semiconducting SWCNT acts as the active layer in thin film transistors as shown in Figure 28.

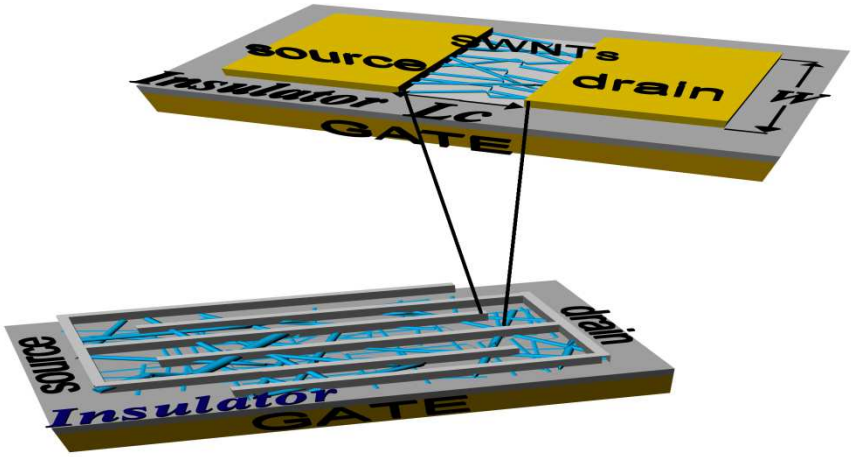

Figure 28. Schematic of SWCNT-TFT as a back gate transistor build on thin film SWCNTs on interdigiated electrodes (IDEs). Upper part shows the one period of structure.

Spatial arrangement of SWCNTs network in the channel of a TFT structure is assessed by scanning electron microscope (SEM) and is shown in Figure 29. It can be observed that drain and source electrodes are connected by SWCNTs forming the thin layer on the substrate.

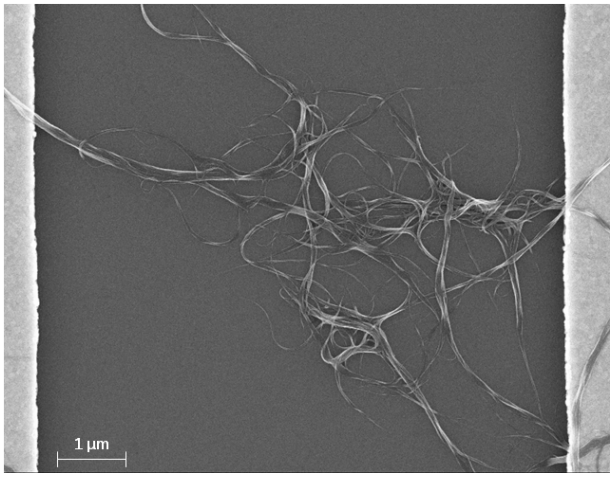

Figure 29. SEM image of SWCNTs network on TFT structure

The electrical characterizations are based on the conventional I-V equations for MOS devices in triode and saturation regime. The classical equations describe the I_{DS} current that flows from the drain to the source in a p-type MOSFET [132]. In the triode region, i.e. $V_{DS} > (V_{GS} - V_{th})$, where V_{th} is the threshold voltage, the current is given by:

$$I_D = -\mu C_G \frac{W}{L_C}\left((V_{GS} - V_{th})V_{DS} - \frac{V_{DS}^2}{2}\right) \quad (8)$$

where L_C is the channel length, W the channel width and C_G the capacitance per unit area between the gate electrode and the nanotube network. If the saturation region is taken into account, i.e. $V_{DS} < (V_{GS} - V_{th})$, the drain current in a p-type MOSFET is governed by the following equation:

$$I_D = -\frac{1}{2}\mu C_G \frac{W}{L_C}(V_{GS} - V_{th})^2 \quad (9)$$

where the C_G is the capacitance per unit area between gate and nanotube network used in equation (8) and (9) which is obtained by considering a parallel plate arrangement:

$$C_G = \frac{\varepsilon_0 \varepsilon_r}{t_{ox}} \quad (10)$$

where $\varepsilon_0 = 8.854 \times 10^{-12}\ F/m$ is the vacuum electric permittivity, $\varepsilon_r = 3.8$ is the relative permittivity of the SiO_2 substrate and $t_{ox} = 100$ nm is the thickness of the oxide.

In Figure 30 the measured electrical characteristics of 90% semiconducting SWCNTs-TFT for channel length L_C= 50 μm is reported. In order to obtain the transfer and output characteristics of SWCNTs-TFT, a standard two probe measurement was made to evaluate the drain current based on modulation of the gate voltage. The sample placed on a probe-station where needles are used to contact the drain and source electrode. The software controls the applied voltages of the the device under the test. The transfer characteristics of device, shown in Figure 30(a), is obtained by varying V_{GS} between $-20\,V$ to $15\,V$ at $V_{DS} = -1\,V$. In order to

measure the output characteristic of the transistor, V_{DS} is varied between -20V to 0 V and V_{GS} between -17V to -1 V with a step size of 4V.
The output characteristic of device is shown in Figures 30(b).

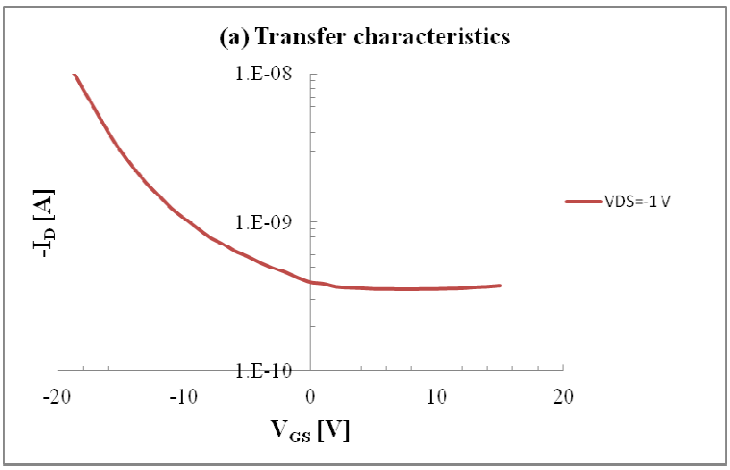

(a)

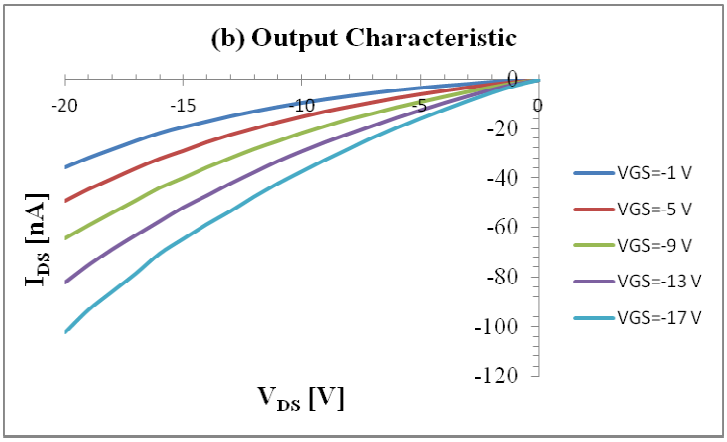

(b)

Figure 30. Transfer (a), and output (b) characteristics of 90% semiconducting SWCNTs-TFT at channel length , L_C= 50 µm

The manufactured devices ($L_C = 50\,\mu m$ and $W = 20\,mm$) showed output performances of typical SWCNTs-TFT. The transfer curve in Figure 30a shows the dependence of charge carrier concentration in thin film of SWCNTs based on electric field and gating effect of the Schottky barriers at the SWCNTs and gold contacts [133]. Also, transfer curve shows the p-type semiconducting thin film behaviour,

consistent with prior work on nanotube networks [134, 135]. Another figure of merit for SWCNT-TFT structure, if the switching behaviour of the device is considered, is the I_{ON}/I_{OFF}ratio. I_{ON} and I_{OFF} are the values of I_D current when the SWCNTs-TFT is in on and off-state, respectively. As shown in Figure 30(a), the I_{ON}/I_{OFF} was 45 and quite low. The reason is that when the transistor is in the off-state, i.e. there is no gate voltage applied, the current should be zero; however, due to the existence of a metallic contribution of SWCNTs (10%), the current of transistor does not completely become zero but has a small value. On the other hand, the transistor is switched on when negative gate voltage and drain-source voltage are applied to the device at the same time. The reason is that, when the voltage is applied to the gate electrode, charge carriers (holes) are induced in the semiconducting SWCNTs which facilitate the current flow from drain to source.

The Figure 30b shows the output characteristicof the device. Under more negative V_D, the device exhibits saturation behaviour. However, due to the existence of metallic SWCNTs, the device does not show a pure saturation regime and the current still increases while applying more negative voltage.

The width–normalized electrical resistance in the on-state ($R_{on} * W$) versus channel length is shown in Figure 31.

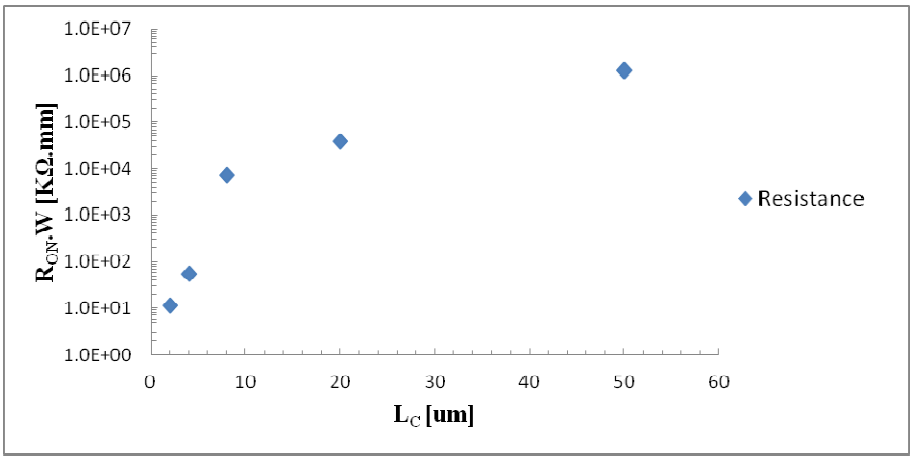

Figure 31.Measurement of width-normalized resistance of 90% semiconducting SWCNTs-TFTs response with different channel lengths. The channel lengths are 2, 4, 8, 20, 50 µm and channel width are 20, 60, 30, 8, 20 mm respectively. The resistance measurement was made on at V_{DS}=-1V and gate bias -20 V (on-state of SWCNTs-TFTs).

As seen from Figure 31 the resistance increases as channel length increases, since the average length of SWCNTs is shorter than channel length and then more SWCNTs were required to form a conduction path from drain to source electrode. Therefore, more tube to tube junctions are present in the conduction path and thus the resistance of devices are limited by the percolative transport through the carbon nanotubes network.
Mostly in devices with shorter channel lengths, the output characteristic shows the short circuit condition because of the metallic carbon nanotubes contribution in the network. This condition occurs if the density surpasses the percolation threshold. On the other hand, in long channel transistors the metallic contribution causes a low I_{ON}/I_{OFF} ratio. Therefore, high percentage of semiconducting SWCNTs solution is demanded to have higher yield of devices. In next section, the fabricated devices with higher percentage of semiconducting SWCNTs will be discussed.

3.2 Experimental process for fabrication of Thin Film Transistors by 99% pure Semiconducting Singe Walled Carbon Nanotubes

In this section, the fabrication process of SWCNTs-TFTs based on 99% pure semiconducting SWCNTs solution and the electrical characterizations will be discussed.

3.2.1 Deposition Process and surface characterization

In order to fabricate thin film transistors with higher semiconductor purity, a 99% semiconducting SWCNTs solution was purchased from NanoIntegris Co. It is supplied with concentration 0.01 mg/ml in surfactant solution, with average length $L_{SWCNT} = 1\ \mu m$ and average radius $r_{SWCNT} = 0.7\ nm$. [136]. A Si/SiO_2 with 100nm oxide layer wafer was used as substrate where SiO_2 is used to act as the back gate dielectric same as previous ones. The drain-source electrodes as explained in section 3.1.1 are interdigitated electrodes (IDEs) with

channel length between $2\,\mu m$ to $50\,\mu m$. Also an effective method (which is a combination of a silanization process and vacuum filtration) was used to deposit the SWCNTs solution onto the substrate. The process is explained in detail in section 3.1.4.
Figure 32 (right) shows the optical image of the source and drain electrodes obtained by IDE, whereas the network of SWCNTs by scanning electron microscopy (SEM) image deposited on it is shown on Figure 32 (left). The Figure 32 confirms connection of drain and source by means of a quite uniform SWCNTs network- film.

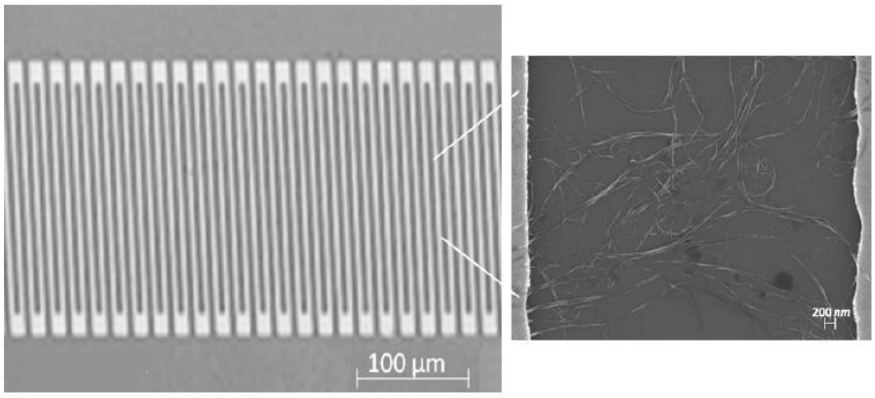

Figure 32. Optical image of interdigited electrode (IDE) as a drain-source electrode (Left). SWCNTs network between one period of IDE (Right).

The morphological arrangement of SWCNTs shown by SEM confirms that drain-source electrode is joined by SWCNTs crossing associated to the random network. This allows application of the percolation theory of a random distribution of conducting sticks due to the fact that nanotubes appear randomly oriented. The percolation theory and modelling of device will be discussed in Chapter4.

3.2.2 Electrical characterization of 99% semiconducting SWCNTs-TFTs by vacuum filtration deposition

Systematic studies of the electrical performances of the SWCNTs-TFTs have been carried out. As many carbon nanotubes deposited in the channel of TFT structure were not involved in the current carrying

process, the classical equations describing the drain current, I_D (equation 8 and 9) modified by scaling law (α) in all regimes (triode and saturation) of transistor are used. This power law (α) is characterized by a unique constant which is based on the coverage density of carbon nanotubes in the channel of the TFT structure [137] and gives the information about the morphology arrangement of carbon nanotubes network on the surface [138]. More details about this power law will be discussed in chapter 4.
In the triode region ($V_{DS} \geq (V_{GS} - V_{th})$) the I-V curve should scale as [74, 137]:

$$I_D = \mu W C_G \frac{1}{L_{SWCNT}} \left(\frac{L_{SWCNT}}{L_C}\right)^{\alpha} \left((V_{GS} - V_{th})V_{DS} - \frac{V_{DS}^2}{2}\right) \tag{11}$$

where C_G is the gate capacitance per unit area, V_{GS} is the gate-source voltage, V_{th} is the threshold voltage, and μ is the mobility. The mobility can be obtained from the transfer characteristic by the derivative of (11), i.e. from the variation of the drain current with respect to the gate-source voltage in the triode region:

$$\mu = \gamma \frac{\partial I_D}{\partial V_{GS}} \tag{12}$$

where the coefficient γ takes into account all the constant terms of the equation 11. Therefore, the mobility of the thin-film transistor based on SWCNTs network can be obtained by using measured values of transconductance of the obtained device, $g_m = \partial I_{DS}/\partial V_{GS}$ and considering its geometry. The gate capacitance (C_G) is calculated by taking into account the electrostatic coupling between carbon nanotubes and oxide where the nanotube is considered as equipotential [139]:

$$C_G = \left\{C_Q^{-1} + \frac{1}{2\pi\varepsilon_0\varepsilon_{ox}} \ln\left[\frac{\Lambda_0}{r_{SWCNT}} \sinh\left(\frac{2\pi t_{ox}}{\Lambda_0}\right)\right]\right\}^{-1} \Lambda_0^{-1} \tag{13}$$

ε_0=8.854×10^{-14} F/cm is the electric permittivity of vacuum, $\varepsilon_{ox} = 3.8$ the relative permittivity of the SiO_2 substrate with thickness $t_{ox} = 100\ nm$, Λ_0^{-1} is the linear tube density. Particularly, C_G from equation

13 is used for aligned SWCNTs and gives a quantitative index [53, 54, 140]. However, when the distance between carbon nanotubes is similar to the dielectric thickness, the use of the gate capacitance from equation 13 instead of that corresponding to parallel electrodes (equation 10) can be adequate [54]. The linear density of carbon nanotubes is about between $10 - 100\ tube/\mu m$ from SEM image; it has been assumed to be $10\ tube/\mu m$ in this case with radius of SWCNT equal to $0.7\ nm$. C_Q is the quantum capacitance which is equal to $4 \times 10^{-12}\ F/cm$ [141]. Therefore the mobility of the SWCNTs-TFT is a function of the SWCNTs network through $C_G = 21 \times 10^{-9}\ F/cm^2$ (expression (13)) and the measured $g_m$value. In fact, the oxide capacitance based on the parallel plate model (equation 10) is used for a uniform film; however, the nanotubes network is not completely uniform and it is represented by a sparse network. Therefore, the oxide capacitance in equation 10, underestimates the mobility of SWCNTs network or overestimates the oxide capacitance. Hence, equation 13 is necessary to compute the real mobility of the device.

A standard two probe measurement was made to evaluate the DC resistance of the channel between the gold contacts of the fabricated devices. The software controls the voltage of the device under test. By varying V_{GS} between $-15\ V$ to $15\ V$ at $V_{DS} = 1\ V$, transfer characteristics of a device is obtained which is shown in Figure 33a. Also, by performing a sweep of V_{DS} between -16V to 0 V and V_{GS} between -10V to 10 V with a step size of 2V the output characteristics of device are evaluated and shown in Figures 33b-c (linear and saturation response of the transistor are obtained, respectively).

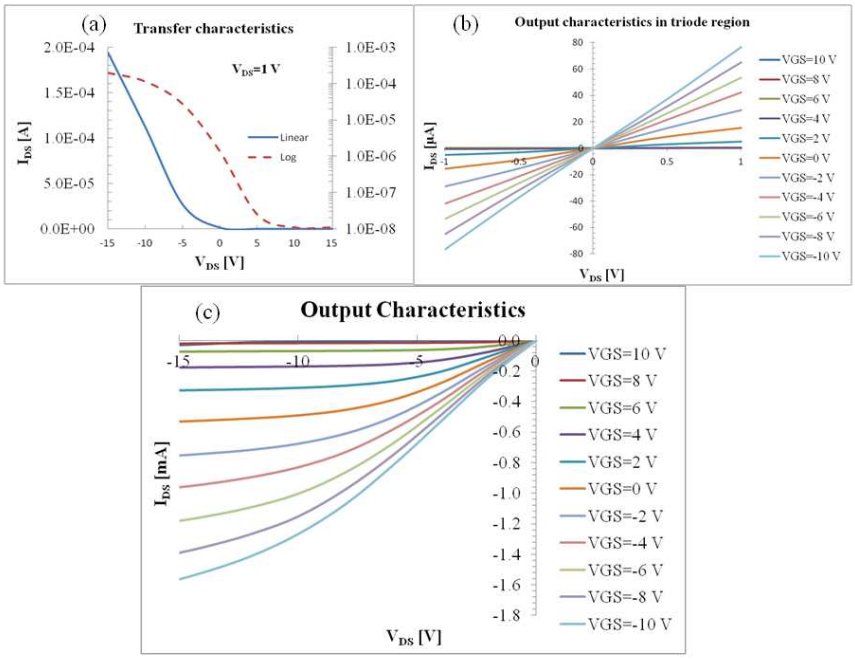

Figure 33. Electrical measurement of a SWCNTs-TFT with channel length L_C=8 μm: a) Transfer characteristics b) Output characteristics in triode region c) Output characteristics in saturation region

The manufactured device ($L_C = 8\,\mu m$ and $W = 30\,mm$) shows output performances of typical SWCNTs-TFT. The transfer curve in Figure 33a shows the dependence of charge carrier concentration in a thin film of SWCNTs based on electric field and gating effect of the Schottky barriers at the SWCNTs gold contacts. Also, the transfer curve shows the p-type semiconducting thin film behaviour, consistent with prior work on nanotube networks [53, 54]. The experimental transfer curve is used to extract V_{th}, on-current density ($J_{on} = I_{on}/W$), I_{ON}/I_{OFF} ratio and mobility. The obtained device is characterized by $V_{th} = 4.8\,V$, I_{on}/I_{off} ratio as high as 1.8×10^4, and sub-threshold $S = d(V_{GS})/d(\log I_{DS})$ equal to 1.8 V/dec at V_{DS}=1 V. In addition, the on-current at V_{DS}=1 V is 190 μA which, to the best of the authors' knowledge, is the highest on-current for fabricated devices based on high purity semiconducting carbon nanotubes network. This high on-current is due not only to the high purity of semiconducting SWCNTs, but also to the electrode design. Furthermore, the mobility of device (μ) is equal to 40.75 cm^2/Vs at V_{DS}=1 V. As shown in

Figure 33b, the I_D-V_D curves appear to be linear for V_D between -1 and 1 V, stating that good ohmic contacts are formed between the interdigitated electrodes and the carbon nanotubes thin film. In this region the TFT behaves like a voltage controlled resistor similarly to the classic MOSFET devices. Under more negative V_D, these devices exhibit complete saturation behaviour, as shown in Figure 33c.
The mobility of 99% semiconducting random network CNT-TFT, is much higher than the typical mobilities of organic TFTs $0.98\ cm^2/Vs$ [142], amorphous Si $1\ cm^2/Vs$ [143], and those reported until now around $1\ cm^2/Vs$ for random network of carbon nanotubes [48, 55, 144]. Moreover, the mobility for $L_C = 8\ \mu m$ TFT structure is 40.75 cm^2/Vs which, to the best of the authors' knowledge, is among the highest mobility in short channel structures for fabricated devices based on high purity carbon nanotube network. However, it is significantly lower than those of a single carbon nanotube CNT-FET ($\mu \sim 1 - 2 \times 10^3\ cm^2/Vs$) [144]. The reason for this difference is the high tube-tube coupling resistance in the films [145]. This intertube coupling resistance is deemed to be as high as 100 MΩ [146], which overcomes the resistance of nanotube ($\sim 10\ k\Omega$). In addition, as it can be seen from the SEM image in Figure 32, curling of carbon nanotubes appears and this phenomenon reduces the effective length of SWCNTs in the direction of the current flow from drain to source electrode, thus increasing the resistance of the dispersion of carbon nanotube network and reducing the overall device mobility.

3.2.3 Effect of Channel Length of 99% semiconducting SWCNTs-TFTs

To get a more comprehensive understanding of device characteristics, the measured normalized on-current density (I_{on}/W) scaled with various channel length between $2\ \mu m$ and $50\ \mu m$ is shown in Figure 34.

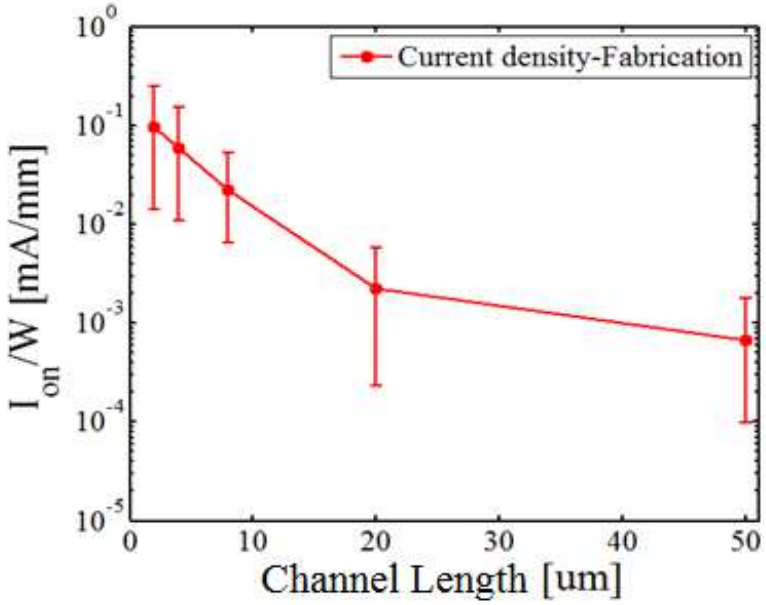

Figure 34. Average values and error bars of the current density (I_{on}/W) versus various channel length (2,4,8,20,50 μm) for TFT fabricated with SWCNTs .

Figure 34 shows the average normalized on-current densities (I_{on}/W) evaluated at $V_{DS} = 1\,V$ and $V_{GS} = -15\,V$ concerning electrical measurements performed on a set of 15 transistors characterized by different channel lengths and widths. The on-current density is approximately inversely proportional to the channel length, indicating that I_{on} decreases as channel length increases because of the enlarged intertube junction resistance. For this reason, the highest on-current density is detected in correspondence of the device with the smallest channel length. Furthermore, as the authors of ref. [147] suggest, higher purity semiconducting nanotubes require more ultracentrifugation which gives rise to shorter nanotube lengths. This effect causes more tube-tube junction in the percolation path and adversely affects the overall on-current density.

Another important figure of merit for SWCNT-TFTs, the average mobility of devices with various channel lengths, is plotted in Figure 35.

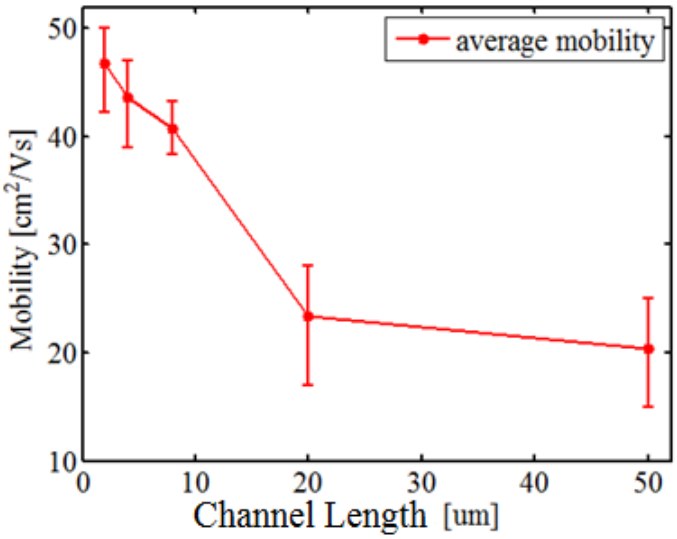

Figure 35. Plot of average mobility versus channel length for TFT fabricated on carbon nanotubes.

The mobility of devices should be related to the bulk property of the device (independent of TFT channel length and width), due to the presence of metallic nanotubes and percolation effect [54]. However, it has been usually observed that the mobility does in fact depend on channel length in as-grown nanotube networks, containing 1/3 metallic and 2/3 semiconducting nanotubes [48, 54]. This behaviour has been detected also for networks containing high percentages of enriched semiconducting nanotubes [53, 148] as well as for those investigated in the present study (99%). In fact, it is also found a dependence on channel length of the current density and mobility, as shown in Figures 34 and 35 respectively. The evidence that also mobility is inversely proportional to the channel length indicates that mobility decreases as channel length increases since the average length of SWCNT in separated nanotubes is shorter than the channel length. Therefore the device mobility is affected by the percolative transport through the carbon nanotube network. As the device channel length increases compared to the carbon nanotube length, there are significantly more tube-to-tube junctions introduced in the conduction path, causing the device mobility to decrease.

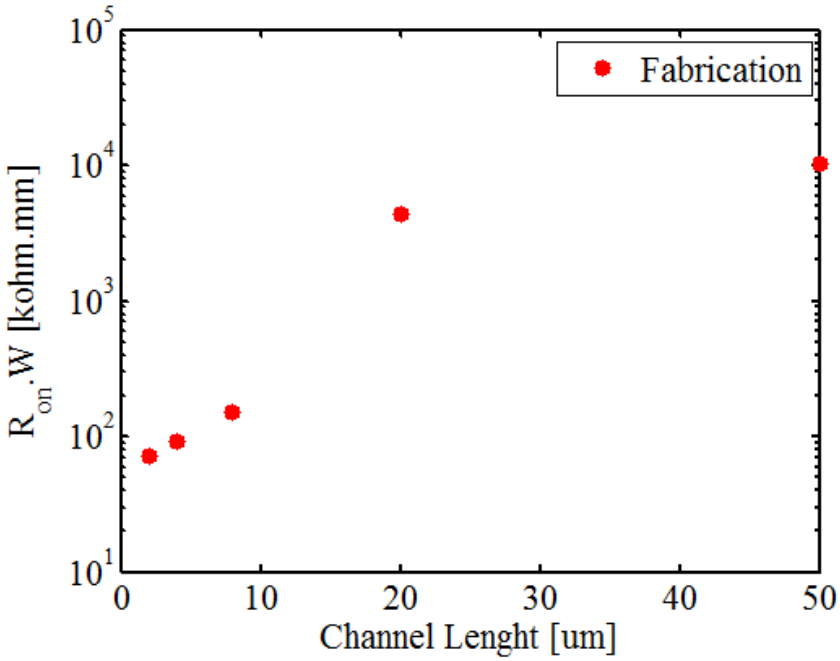

Figure 36. Measurement of width-normalized resistance of 99% semiconducting SWCNTs-TFT response with different channel lengths. The channel lengths are 2, 4, 8, 20, 50 µm and channel width are 20, 60, 30, 8, 20 mm respectively. The resistance measurement was made at V_{DS}=1V a gate bias -15 V (on-state of SWCNTs-TFTs)

The width–normalized electrical resistances of on-state ($R_{on} * W$) devices versus channel length are shown in Figure 36. As seen from Figure 36, the resistance increases as channel length increases, since the average length of SWCNT is shorter that channel length. Therefore the device resistance is governed by the percolative transport through carbon nanotubes network in the transistor channel.

Chapter 4

Numerical modelling of SWCNTs-TFTs

In order to understand the relation linking the electrical properties of fabricated SWCNTs-TFTs with the corresponding geometrical structure and physical characteristics of the nanotubes, a numerical model of the system has been developed. For this purpose, a model simulating a channel of TFT structure with SWCNTs network has been carried out by considering, in a three-dimensional (3D) space, a random distribution of impenetrable conducting cylinders inside the channel. The characteristics of the fabricated devices have been compared with the 3D model and the results are analysed.

4.1 3-D Modelling of SWCNTs-TFTs

The physical representation of the device given in Figure 20 can be described by considering each periodic part reported in Figure 37. In this figure the SWCNTs network acts like an electrical equivalent medium with electronic characteristics dependent on the physical interactions at the interface between nanotubes in the percolation-path, if it exists, that are influenced by external electrical field. In particular, the electrical percolation path connecting drain and source electrodes highlighted by red-sticks involves not all the SWCNTs deposit in the TFT channel. In order to reproduce the transport properties of the SWCNTs network formed in the channel of the TFT, the randomly-generated 3D SWCNTs structure between the two electrodes shown in the schematic zoom of Figure 37 is considered.

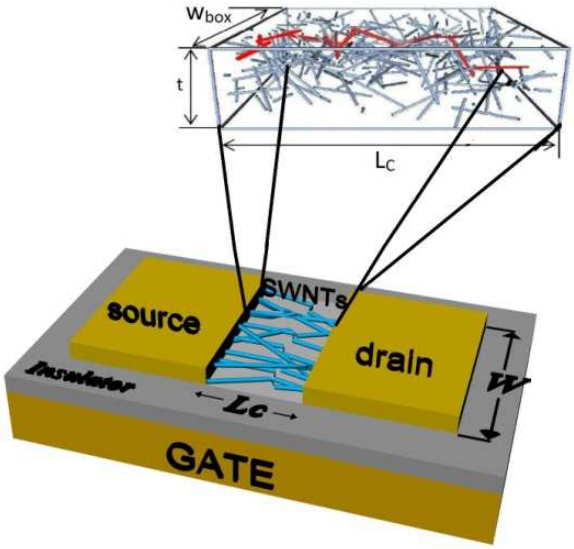

Figure 37. Schematic of SWCNTs dispersion in the channel of TFT as parallelepiped volume form

The conduction mechanisms occurring between the SWCNTs forming the network are evaluated by using an equivalent resistance representation of the selected box, as shown in Figure 38, capable to furnish the electric equivalent medium of the system.

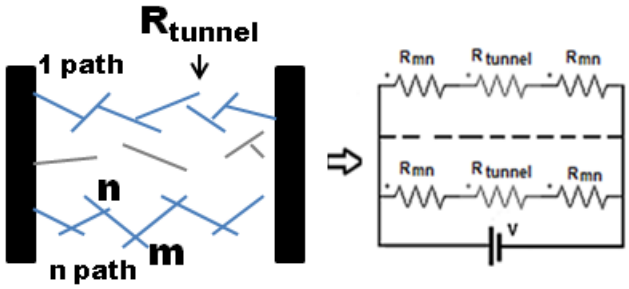

Figure 38. 2D view of the conductive paths inside the channel of TFT and the associated resistor network

Several authors have proposed the study of this problem by considering a physical arrangement of the SWCNTs network in 2-

dimensional (2D) model [74, 149]. Due to the role assumed by the geometric characteristics of the SWCNT and their effect on the device behaviour, a 3D study of the problem is adopted, based on the previous work [150, 151]. In particular, a MATLAB® based procedure has been developed to generate the random deposition of the nanotubes inside the TFT channel represented with parallelepiped shape with fixed volume. The aggregation of SWCNTs takes place in this volume. From the information about the relative position of the SWCNTs inside the volume, an equivalent electrical network is constructed, modelling the conduction mechanism inside the paths that occur in this volume. By using the assumption that the current flows from the source to drain, the equivalent total resistance can be computed by considering the equivalent network of resistances that concurs to form the total path between the drain and source electrodes (sect. 4.1.2). Crucial point will be N_C, the minimum number of SWCNTs connections allowing the formation of conduction path [152]. For the random distribution of the nanotube network, this critical surface density is given by [138, 153]:

$$L_{SWCNT}\sqrt{\pi N_C} = 4.236 \qquad (14)$$

Based on the L_{SWCNT} value obtained from data sheet, the computed critical density is $\mathrm{N_C} = 5.71\ \mu m^{-2}$. It is found that a nanotube density in the TFT channel $\mathrm{N} = 10\ \mu m^{-2}$ is sufficient to achieve a numerical convergence and therefore it is adopted in this simulation approach.

4.1.1 Representation of the SWCNTs aggregation

In order to reproduce the electrical resistivity of the randomized network representing the thin layer in the structure of Figure 37, a representative volume with a parallelepiped shape, V_{box} named cell, is considered. The dimensions of the cell are chosen according to the TFT structure shown in Figure 37:

$$V_{box} = L_c \cdot t \cdot W_{box} \qquad (15)$$

where L_c and t are the channel length and minimum thickness of the channel in the device, whereas W_{box} is fixed to 10 μm. In this way the total volume of the TFT structure, V_t, is given by subdividing the channel width W (and hence the volume) into $n = W/W_{box}$ elementary parts, as shown in the zoom reported in Figure 37:

$$V_t = L_C \cdot t \cdot W = L_C \cdot t \cdot W_{box} \cdot W/W_{box} = V_{box} \cdot W/W_{box} = nV_{box} \qquad (16)$$

Therefore, by assuming periodic boundary condition, the computational effort can be reduced.
In the V_{box} a distribution with uniform probability of cylinders modeling SWCNTs is considered by the adopted N. In particular, each cylinder has a length L_{SWCNT} and diameter d_{SWCNT}. Moreover, in order to ensure that the dispersed SWCNTs are distributed uniformly inside the volume, the initial and final coordinates (x_i, y_i, z_i) and (x_f, y_f, z_f) respectively are used by considering the following analytical relations [150, 151]:

$$x_i = rand_1 \cdot L_C, \qquad y_i = rand_2 \cdot W_{box}, \quad z_i = rand_3 \cdot t, \tag{17}$$

$$x_f = x_i + L_{SWCNT}\emptyset_1 \cos(\mu_1), \; y_f = y_i + L_{SWCNT}\emptyset_1 \sin(\mu_1), \; z_f = z_i + L_{SWCNT}\vartheta_1 \tag{18}$$

In the above equations the parameters $\emptyset_1, \mu_1, \vartheta_1$ are related to the angular distribution defined as follows:

$$\vartheta_1 = 1 - 2 \cdot rand_4, \quad \emptyset_1 = \sqrt{1 - {\vartheta_1}^2} \qquad \mu_1 = 2\pi \cdot rand_5 \tag{19}$$

where $rand_i$, for i=1,…, 5 are uniformly distributed random numbers in the interval $Y = [0,1]$. In this way each Monte Carlo trial corresponds to the generation of 5 uniformly distributed parameters that have to respect some constraints. In fact, during the generation process for inserting the cylinders, a rigorous check regarding contact is performed. In particular, the position or overlap of each SWCNT is essential for the correct determination of the percolation paths. Therefore, at each time, before inserting the new cylinder, a control is made to satisfy the physical feasibility, i.e. that the new cylinder does not penetrate inside others. A further check is also made on the minimum distance between two SWCNTs, by considering the Van der Waals separation (0.34 nm). If this two constrains are not satisfied, the cylindre is automatically removed from volume and a new one is generated again until the conditions are satisfied. This generation procedure is finished when the SWCNTs have reached a number related to the density N established at the beginning of process.

4.1.2 Electrical resistance of the thin-film by means of an equivalent electrical network

Once the structure is obtained, i.e. the cell filled with a network of semiconducting SWCNTs, the presence of one or more direct paths between source and drain electrode can be evaluated. Then the resistance of a nanotubes network in the on-states can be calculated by using a 3D resistor network. It leads to evaluate the resistance of V_{box}, R_{box}, and to derive the equivalent electrical properties of the medium in the channel direction. Each branch in the equivalent circuit represents a single percolation path including two types of resistors. The first one, "tube segment" R_{mn}, takes into account the conductive mechanism in the segment, defined from n to m, of the SWCNTs involved in the path:

$$R_{mn} = \rho_{SWCNT} \cdot \frac{l_{mn}}{S_{SWCNT}} \tag{20}$$

where ρ_{SWCNT} and S_{SWCNT} are the electrical resistivity and cross-sectional area of the SWCNTs respectively, while l_{mn} is the distance between two generic points m and n. It corresponds to assume that the scattering dominated drift-diffusion theory applies, with negligible effect of the diffusive term, and that the contact resistance is unimportant [154]. In particular, the resistivity of the semiconducting SWCNTs is computed, according to the experimental data, as:

$$\rho_{SWCNT} = 1/(n_p e \mu) \tag{21}$$

where $n_p = n_e = 7 \times 10^{18}\ cm^{-3}$ is the charge density of graphene [155], $e = 1.6 \times 10^{-19}\ C$ is the electric charge of electron and μ is the mobility of charges in TFT structures, obtained experimentally as described in the section 3.2.2. For the minimum contribution of metallic nanotubes (1%) in the network, the resistivity of them, in on-state, is adopted equal to that of the semiconducting CNTs [53]. Moreover, in the proposed electrical network a second type of resistor, R_{tunnel}, is introduced at each "tube-tube" junction in order to take into account electron tunneling effect between sufficiently close carbon nanotubes [156-158]:

$$R_{tunnel} = \frac{h^2 d}{S_{SWCNT} e^2 \sqrt{2 m_e \lambda}} exp^{(\frac{4\pi d}{h}\sqrt{2m\lambda})} \tag{22}$$

where h is the Plank´s constant , d the distance between SWCNTs, m_e the mass of electron and λ represents the height of energy barrier. As a first approximation, it is assumed that the barrier height approximately equal to 1/2 band gap of the semiconducting SWCNT [159].

From the above expression, it can be noted that tunnelling conductance decays exponentially as a function of distance with a characteristic decay length in the order of a few nanometers, typically not larger than $2nm$ [157]. Finally the equivalent resistance of all paths in parallel R_{box} associated with the conduction mechanisms is given by:

$$R_{box} = \left(\sum_{l=1}^{K} \frac{1}{\sum_{i=1}^{P} R_{mni} + \sum_{j=1}^{M} R_{tunnelj}} \right)^{-1} \quad (23)$$

where index of summation *K* is the number of the parallel percolation paths detected in the thin film, *P* and *M* are respectively the number of SWCNTs and tunnelling occurrence in each branch of the resistor network.

The on-state resistance (R_{on}) indicates the total resistance ($R_{on} = R_{box}/n$) of the transistor when it is in the conduction state.

In classical 2D conducting film, the R_{on} is proportional to channel length, L_C. In a system close to percolation threshold, there are many nanotubes that are not involved in the current carrying process [137]. These tubes lead to form new percolation paths as L_C decreases. Therefore, the on-resistance can be expressed quantitatively according to [74]

$$R_{on} \sim L_{SWCNT} \left(\frac{L_C}{L_{SWCNT}} \right)^{\alpha} \quad (24)$$

α is universal constant which depends only on the normalized density ($N{L_{SWCNT}}^2$) of SWCNT in the transistor channel and describes the spatial distribution of SWCNTs network in the structure. In addition, this power law gives the information about dimension of morphology arrangement of carbon nanotubes network on the surface [137, 138].

4.1.3 Simulation result of electrical properties of SWCNTs-TFTs

For a better understanding of the relation linking the electrical properties with the geometrical and physical characteristic of the SWCNTs-TFT, a comparison between the characteristics of the fabricated device with a 3D model of the structure, obtained by

randomly distributed carbon nanotubes inside a TFT channel length, is performed.
The transport properties of the SWCNTs network in the TFT channel are modelled in terms of stick percolation on the 3D structures leading to the formation of conduction paths between source and drain as discussed in section 4.1. In Figure 39 the box representative of a random arrangement obtained in the case of a parallelepiped volume with $L_C = 8\ \mu m$, $W_{box} = 10\ \mu m$ and $t = 3.14\ nm$ is reported.

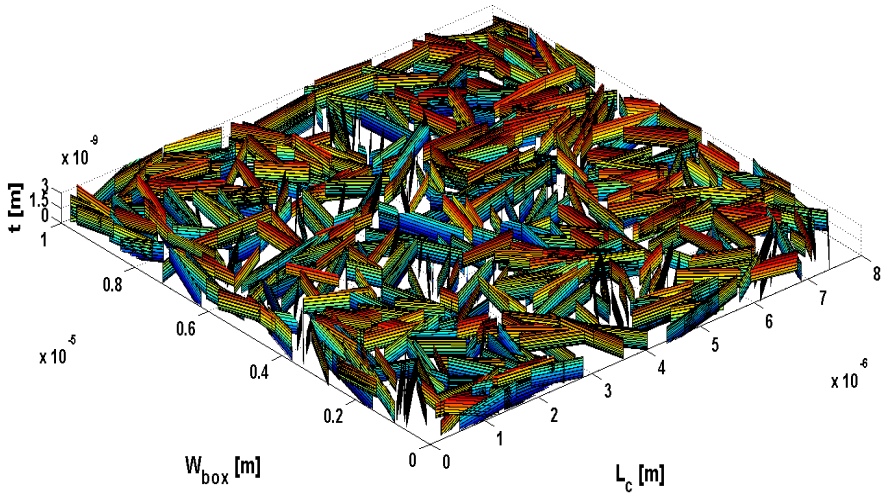

Figure 39. 3D simulated box representing the random network of 800 SWCNTs inside the TFT channel Lc

The thickness value is adopted in order to consider that two carbon nanotubes can overlap each other according to their diameter and Van der Waals distance. In all TFT structures, the average nanotubes length L_{SWCNT} is shorter than the channel length, L_C, which means that source to drain current has to flow through a series of inter-nanotubes contacts. The SWCNT geometric characteristics are adopted according to the data sheet (length $L_{SWCNT} = 1\ \mu m$ and radius $r_{CNT} = 0.7\ nm$) and they are randomly inserted in the box, one at time, until the desired density is reached. A resistor network is associated to the "tube segment" and "tube-tube junction", as explained in section 4.1.2. The resistivity of SWCNTs network based on the variation of devices mobility are obtained by experimental data and varying between $2 \times 10^{-2}\ \Omega cm$ to $4 \times 10^{-2}\ \Omega cm$ according to eq. (21). These ranges of resistivities are consistent with those

obtained from recent publication [160, 161]. Finally the total resistance of the box, R_{box} of device is derived by means of the Equation (23). The simulated values of the geometrically-scaled devices resistance in on-state of transistor ($R_{on} * W$) are compared with the measurement data in Figure 40.

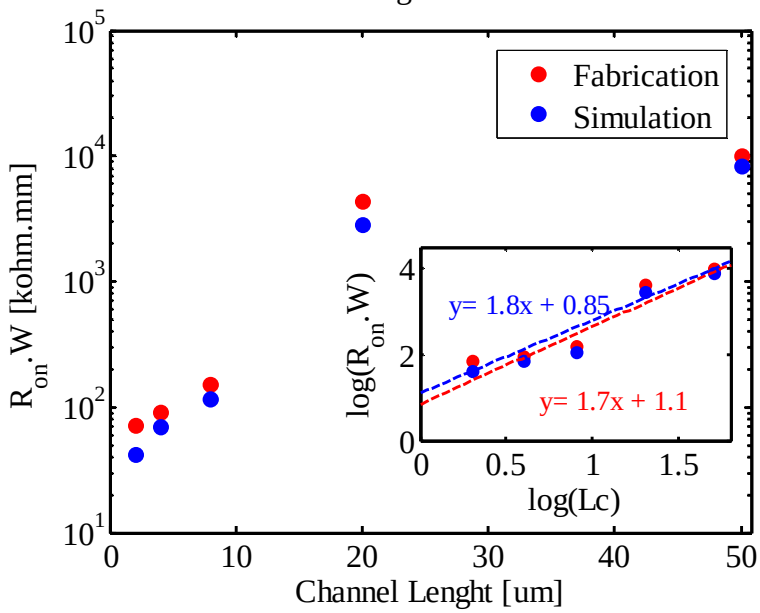

Figure 40.. Comparison between measurement and simulation of width-normalized resistance of semiconducting devices response with different channel lengths. The channel lengths are 2, 4, 8, 20, 50 µm and channel width are 20, 60, 30, 8, 20 mm respectively. The resistance measurement was made at V_{DS}=1V a gate bias -15 V (on-state of SWCNTs-TFTs) that was applied to ensure that semiconducting nanotubes in the network were conducting. Inset plot shows log of width-normalized resistance [log (*R*W*)] versus log channel length [log(L_c)]

The inset of Figure 40 shows also the plots of the logarithm of the width-normalized electrical resistance of semiconducting response of TFTs $\log(R_{on} \cdot W)$ vs. $\log(L_C)$ at the fixed V_{GS} of -15V, corresponding to an on-state value. From this plot it is possible to extract the exponent power law (α) as the slope of the interpolating line for fabricated and simulated devices. By observing the equations it is evident that $R_{on} \propto (L_C)^{1.7}$ (red data) and $R_{on} \propto (L_C)^{1.8}$ (blue data) respectively.

For high density network, the carbon nanotube network behave like a classical 2D conducting film and correspondingly $\alpha \approx 1$. On the other hand, for densities near the percolation threshold, α approaches 2 and

then diverges as the density approaches zero [66, 137, 154]. In these structures, the detected exponent of the power law $\alpha = 1.7 - 1.8 \in [1,2]$ puts in evidence that the obtained thin film is "quite" dense, with a density higher than the percolation threshold value but still not so high to induce a linear behaviour between resistance and channel length. It means that an intermediate SWCNTs aggregation structure between 2-D and 3-D is achieved and therefore the adoption of 3D model appears to be useful for the numerical investigation of the thin-film structure.

Good agreement between measured and simulated data is clearly visible thus confirming the effectiveness of the model for the design phase of optimized SWCNTs-TFT structures.

Chapter 5

Fabrication label-free biosensor based SWCNTs-TFT

Detection of biomolecules by fast, sensitive and cost effective methods is an important issue for several sectors such as healthcare, food, water, environmental monitoring and elimination of bio-security threat [56, 162]. Various detection methods ranging from conventional approaches such as optical detection by utilization of fluorescent-labeled biomolecules with dyes [163-165] or quantum dots [166-168] to the sophisticated optical fiber based evanescence wave biosensor and polymerized chain reaction (PCR) based method have been developed so far[56, 148, 169, 170]. Although the labelled biomolecule approach has an accurate detection, it degrades the interaction between receptor and target [171]. In addition, the preparation of labelled materials is time consuming and expensive [171, 172]. Therefore, the development of a fully electronic label-free biosensor is highly demanded. Label-free biosensors with high miniaturization, high sensitivity and low power consumption have drawn interest into the field of nanoscience and nanotechnology [62, 173, 174]. The integration of nanotechnology and biotechnology provides new routes for the detection of specific biomolecules through detection of electrical signals [175].

Among nanomaterials, single walled carbon nanotubes (SWCNTs) are promising candidates for nanobiosensing due to the exceptional electrical properties such as high mobility [176], large surface area [177], and their nanoscale structure [178]. The high mobility of SWCNTs represents a major advantage for high sensitivity applications [178]. Moreover, in the SWCNTs every single carbon atom on the surface is in direct contact with the environment, allowing

increase of the sensitivity [179]. In addition, the nanoscale size of SWCNTs (with diameter ~1 nm), is directly comparable to the dimension of single biomolecules such as DNA, enzymes, antibodies proteins [67, 179, 180] and enables easy interaction with such biomolecules. Moreover, the low charge carrier density of SWCNTs, ~1 electron per nanometer, is similar to the surface charge density of proteins, allowing optimal electrostatic interaction between SWCNTs and analyte biomolecules [179]. These attractive features of such devices can approach the realization of an ultrahigh sensitivity biosensor capable of single-molecule detection [66]. The translation of the interaction of biomolecules and surface of SWCNTs to an electrical signal is the base of performance of the label-free biosensor. This makes SWCNTs excellent candidates for application as transducers based on chem-resistor or transistor structures [48].

Since the fabrication of field effect transistor based CNTs [181] there has been great deal of effort devoted to the application of this device for various sensing areas from chemical sensors [182], gas sensors [183] DNA sensing [184], and protein sensors [185, 186].

Proteins can strongly attach to the nanotube surface via nonspecific binding due to the affinity to attached amino groups [187, 188]. There are also various reports that demonstrate the specificity and selectivity control for chemically covalent [189] or non-covalent [190] functionalized CNTs [191]. Biosensors based on nanotubes have shown detection range between picomolar to micromolar concentration [185, 192, 193] and potential applicability for large-scale array [192-194].

Hu et al. have been utilized 60% semiconducting SWCNT-TFT for detection of 50 nM concentration of streptavidin [185]. However, they used break-down electrical procedure for removing metallic contribution of SWCNTs network in the system. This additional process is not suitable for large-scale array-ability for biosensors fabrication and reducing the reliability of devices. Because of high bias voltage is required to break-down the metallic species. Chen et al. have been used mixtures of SWCNTs network on mesh gold grids for detection of various biomolecules [190]. They detected 100 nM of streptavidin based on gold labelled particle directly on the surface of SWCNTs network. The streptavidin is binding with the surface of SWCNTs with non-specific binding. Furthermore, labelled biomolecules have the disadvantage to degrade the interaction

between target and receptors. Therefore, a fully electronic-label-free biosensor is demanded. In this work, TFTs based on SWCNTs networks with the highest purity semiconducting (99%) is used for detection of streptavidin at concentration as low as 100 pM via specific binding to biotin.

In this chapter, a label-free biosensor based on the fabricated high purity SWCNTs-TFT is considered as a transducer for bio-interactions. The TFT structure with SWCNTs network as an active layer is used as a platform of sensing mechanism. The electrical conductivity of this device is modulated by the interaction of the functionalized surface of SWCNTs with specific proteins. In particular, the object of this chapter is the description of the fabrication of a high sensitivity (100 pM) biosensor for the detection of streptavidin. The principle used for this detection in based on the well-known biotin-streptavidin interaction. The incubated process for immobilization of biomolecules is inspired by Chen et al. [190] and developed for our application.

5.1 Interaction between biotin-streptavidin

Among the many non-covalent interactions between proteins and receptors present in nature, the streptavidin-biotin interaction is the strongest ($K_d = 10^{-14}$ - 10^{-15} M) where K_d is the dissociation constant [195]. Streptavidin is a tetrameric protein ($4 \times 13\, kDa$) which binds to the vitamin biotin [196]. In fact, the mass of streptavidin is 52000 dalton (Da) or as a short 52 kDa . In other words, streptavidin constructed from four identical subunits and it is represented as ($4 \times 13\, kDa$) and one molecule of streptavidin binds with four molecules of biotin

The bond between that pair is very stable and unaffected by pH, temperature, organic solvents and other denaturing agents [195, 196]. These features make the biotin/streptavidin system the basis of many biochemical and biosensor applications and in this work we have used this pair as a research model for development of a label-free biosensor.

5.2 Immobilization procedure for deposition of biomolecules on SWCNTS-TFT

The fabricated 99% pure semiconducting SWCNTs-TFT, described in section 3.2, is used as a transducer acting as the central element of a biosensor.

Generally, pristine SWCNTs have some shortcoming such as low sensitivity to analytes due to low absorption and non specific adsorption; hence, functionalized CNTs are needed for selective adsorption and to improve the sensing performance. In particular, to improve the sensitivity and selectivity, the SWCNTs in the TFT structure are non-covalently functionalized by submerging the device into a 6mM solution of the linker (1-pyrenebutanoic acid, succinimidyl ester, Eurogentec, Inc.) dissolved in dimethylformamide (DMF) for 1 hour. Then the device is rinsed with DMF solvent.

In order to biotinylate the device, the biotin is immobilized on the pyren-linker present on the SWCNTs surface by submerging it in a 50 mM concentration of EZ-Link Amine-PEG_3-Biotin (Thermo Fischer Scientific, Inc.) in aqueous solution for 18 hours at room temperature and rinsed in pure water for 1 h in order to wash the excess of the reagent. Subsequently, the biotinylated polymer coated device is exposed to a 100 pM solution streptavidin (Omnilab.Inc.) in a 0.02 M phosphate buffered saline solution (PBS) at pH=7.2 and at room temperature for 15 min. Then, the device is rinsed copiously with water to remove salt from saline buffer and dried with a flux of nitrogen. The schematic of the immobilization procedure is shown in Figure 41.

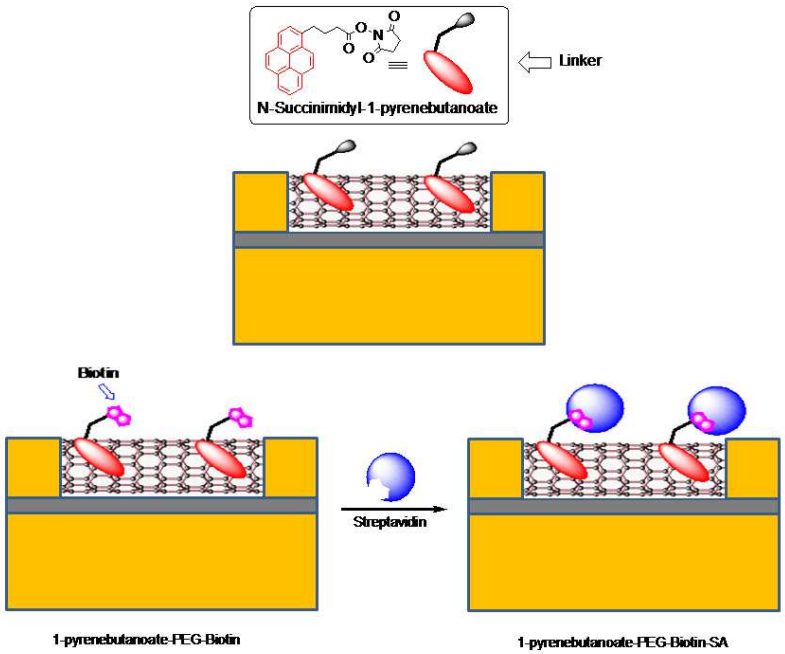

Figure 41. Schematic of immobilization procedures of protein. First deposition linker, second biotin and finally protein (Streptavidin) with 100 pM concentration

5.3 Experimental result for biosensor

TFT with randomized network of 99% semiconducting SWCNTs having channel length, $L_C = 8\,\mu m$ and width, $W = 3\,mm$ on Si/SiO_2 is employed. The biosensor operates in the triode regime of the transistor where the conduction changes as a function of biomolecule interaction. The detection of streptavidin in a concentration of 100 pM is targeted in the experiment.
Figure 42 shows the immobilization of biomolecules on the surface of functionalized SWCNTs.

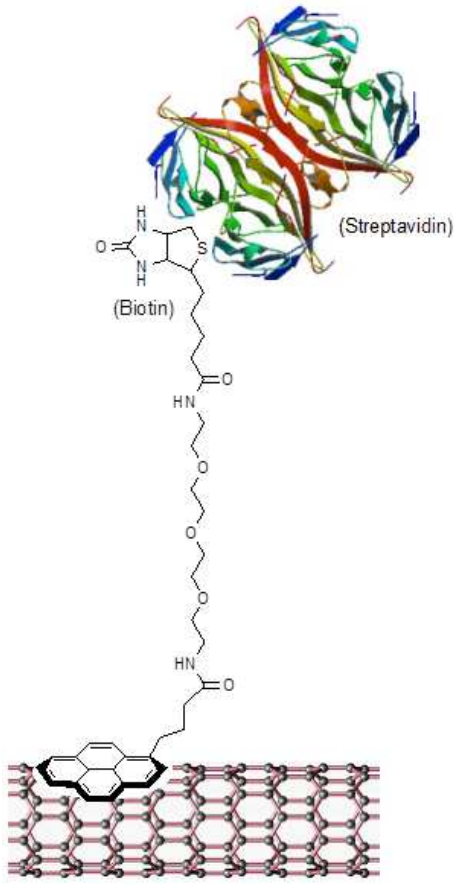

Figure 42. Schematic of SWCNT with immobilization of 1-pyrenebutanoic acid succinimidyl ester as a linker, Amin-PEG-Biotin for biotinylated the device and streptavidin

The biosensor based on SWCNTs-TFT is operated at room temperature in four steps: 1) the bare SWCNTs; 2) SWCNTs with linker; 3) SWCNTs with attached biotin; 4) SWCNTs with streptavidin. The electrical conductance variation is reported in Figure 43.

The main advantage of the noncovalent functionalization is the preservation of the sp^2 carbons present in the nanotube structure. The interaction between nanotube surface and tetracyclic pyrene is due to the non-covalent π-stacking interaction [190]. It must be noted that the observed reduction of the current is related to a partial depletion of holes in p-type SWCNTs by the electron-donating DMF which cover the surface of carbon nanotubes.

The reactive succinimide portion of the pyrene linker adsorbed on the nanotubes is able to induce the formation of a covalent bond with the amine-PEG_3-Biotin. In this way, the biotin is connected to the SWCNTs through an amide bond. Because all the valence electrons present in the atoms constituting the amide group (amide=carboxyl+amino) are for covalent bonds, they cannot act as electron donors. Therefore, the level of conductance of biotinylated SWCNTs-TFT is almost back to the level of the bare SWCNTs in TFT. The short polyethylene glycol (PEG) portion in EZ-Link amine-PEG_3-Biotin is highly hydrophilic, confers high water solubility and, above all, is charge-neutral. All these characteristics eliminate non-specific hydrophobic interaction and electrostatic binding with proteins leading to high degree of detection [186].

As shown in Figure 43b, the current increases sharply upon interaction of 100 pM concentration of streptavidin (target) with the receptor which is biotinylated-SWCNTs-TFT, indicating that the target is detected successfully. The 37% relative increase of the current (upon addition of streptavidin) can be related to the binding of a negatively charged species to the surface of a p-type SWCNTs network. This is in full agreement with the streptavidin isoelectronic point (pI) of about $5\ to\ 6$ and the fact that the exposure the biotinylated-SWCNT surface with streptavidin was done at pH=7.2 (at this pH the streptavidin must have an excess of negative charges) [185, 199, 200]. Therefore, the result indicates that streptavidin is successfully bound to the biotinylated-SWCNTs via biological recognition of the biotin-streptavidin pair. In principle SWCNTs surface in the channel of TFT is a p-type semiconductor and it is expected to increase the current when negative charges come close to its surface [200, 201] . Our result is compatible with this consideration. In addition, our result confirms previous investigations related to interaction between biotinylated-SWCNTs and streptavidin [185, 200]. This high sensitivity is due to the very high (99%) purity percentage of semiconducting SWCNTs and large dimension of IDEs in TFT structure that allow more efficient interaction between the analyte and surface of SWCNTs.

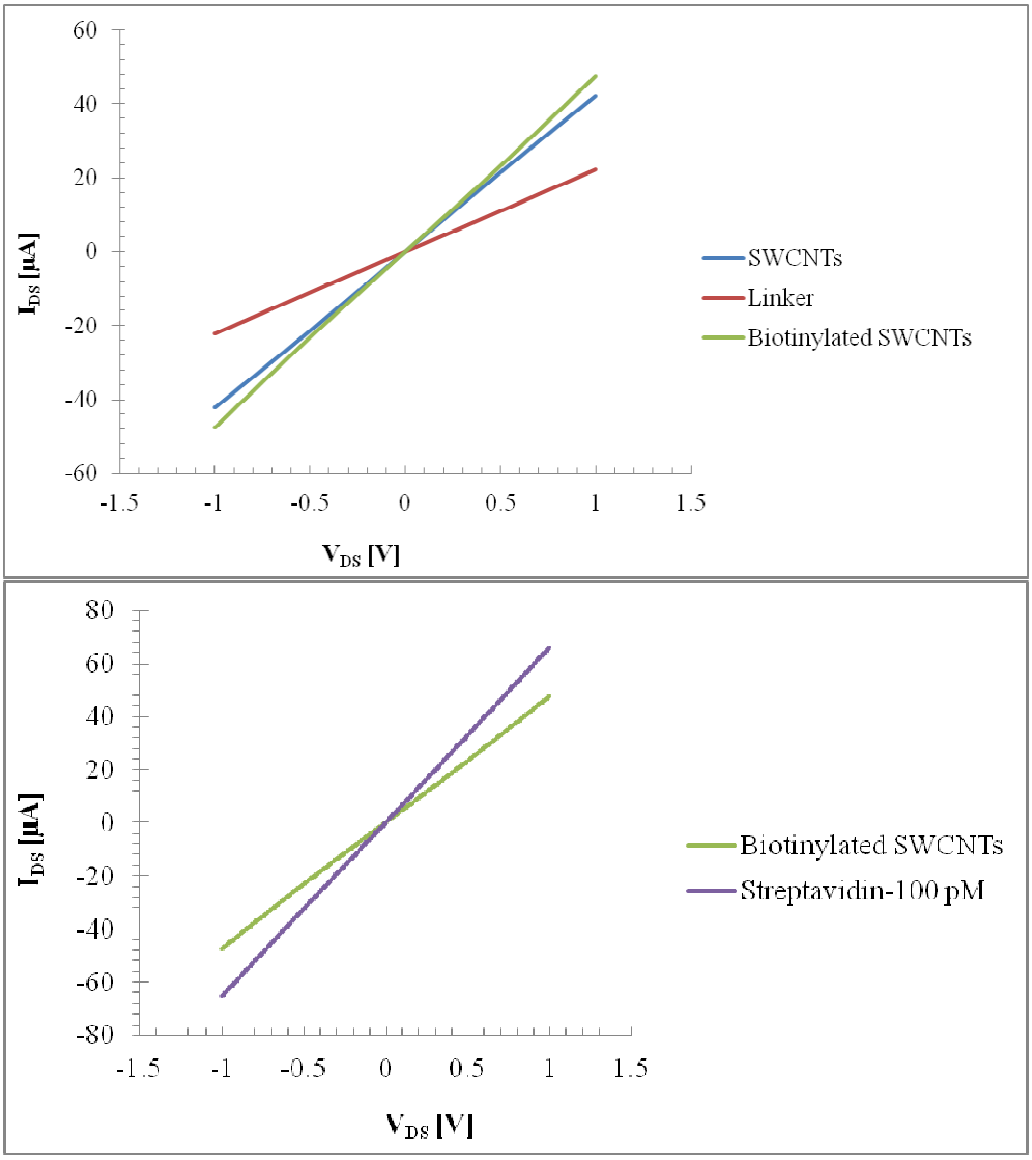

Figure 43. Output characteristics (Ids-Vds) of the SWCNTs-TFT at Vgs=-5 V for: (1) bare SWCNTs-TFT ; (2) functionalized SWCNT with linker; (3) biotinylated SWCNTs-TFT; (4) SWCNTs-TFT with streptavidin

This investigation is a proof of principle to detect the interaction of biotin and streptavidin on SWCNTs surface. It is used as a research model for biosensor application. In order to use this biosensor for

commercial application, it is required more control tests on it such as directly interaction between protein and SWCNTs-surface without biotinylated the device, different concentration of protein, the role of solvents in the analyte medium and utilization of microfluidic channel on top of the device. These control tests are required to completely investigate the comprehensive mechanisms of interaction between SWCNTs-surface and bimolecular systems.

Chapter 6

Conclusion and future work

6.1 Conclusion

In this work the characteristics of SWCNTs-TFTs fabricated by means of an effective deposition technique from a solution of dispersed pre-separated semiconducting SWCNTs on a Si/SiO_2 wafer have been presented. The deposition technique consists of silanization in combination with the vacuum filtration method. The surface treatment used APTES prior to the nanotube deposition in order to facilitate selective deposition of SWCNTs on the substrate. The vacuum filtration gives an opportunity to deposit thin films on a substrate with control of the density of nanotubes in the TFT channel. Moreover, this technique gives an opportunity to fabricate devices at room temperature which is suitable also for temperature sensitive substrates and pre-existing circuit structures. The proposed approach can be easily transformed to large areas leading to a suitable use in industrial applications. The fabricated TFT based on 99% pure semiconducting SWCNTs solution shows a V_{th}=4.8V, a maximum transconductance of 91μS, a current density of $0.06\,\mu A/\mu m$, a large value of mobility of $\mu = 40.75\ cm^2/Vs$ and a I_{on}/I_{off} ratio as high as 1.8×10^4 for a channel length equal to $8\,\mu m$. According to percolation theory, an exponent of the power law $\alpha = 1.7$ was found experimentally, showing that the obtained thin film is “quite” dense and near the percolation threshold. Furthermore the experimental data have been compared to the results of a 3D model simulating the charge transport in the SWCNT structures formed in the TFT channel. The simulation results are in very good agreement with the experimental data. The model seems to be able to reproduce the transport characteristics of the fabricated devices and could be an effective tool to improve the SWCNTs-TFTs structure. Furthermore, the manufactured device has been characterized as a transducer in a label-free biosensor. The results demonstrated the high sensitivity of

the fabricated TFT biosensor based on high purity semiconducting SWCNTs network. The SWCNTs are functionalized via non covalent process to preserve the electronic characteristic of SWCNTs. The conductance of the label-free biosensor increases upon interaction of streptavidin with biotinylated SWCNTs on the channel of TFT structure. This effect can be attributed to the negatively charged biotin-streptavidin combination via electrostatic interaction. This biosensor shows the successful immobilization of streptavidin and highly sensitive detection of streptavidin with concentration as low as $100\ pM$. Due to the high-sensitivity and nanoscale size of SWCNTs, this new biosensor provides great potential for label-free detection of a wide range of bio molecules in applications, such as array based screening.

6.2 Future work

Since the first fabrication of FETs based on SWCNTs, significant progresses has been made. However, many challenges remain for bringing them from prototype to practical application in mass-production with high efficiency in the nanoelectronics industrial sectors. In order to achieve this aim, it is required to address strategies to assemble SWCNTs thin film on substrates for specific application. In fact, carbon nanotubes are produced as a mixture of metallic and semiconductive CNTs with different diameters and lengths [202]. Therefore, in order to use them for practical application, it is needed to sort them based on their electrical characteristics, e.g. semiconducting ones for transistors and sensors and metallic ones for transparent electrodes and interconnection systems. Although, as explained in this thesis, it is possible to sort them in solution by sonication and centrifugation, shortening the carbon nanotubes lengths, causes a reduction of the current density and mobility of the devices. Other issues to be considered are that advanced film-preparation methods are required in order to achieve improved control of density and orientation, as these parameters strongly influence the properties of SWCNT thin films and therefore the output performances of electronic devices. Additionally, specific techniques are required for controlled doping of SWCNTs, for increasing their conductivity, and reducing parasitic contact resistances [60]. Other problems to be addressed, before routine fabrication of electronic devices based on

CNTs, concern the selection of the most appropriate characteristics with reference to the specific application e.g., higher mobility of devices for sensing application and higher on/off ratio of devices for switching blocks for integrated circuits. In fact, trade-off must always be considered between mobility and on/off ratio for the output performance of TFTs based on CNTs, due to the metallic contribution in SWCNTs. Higher density of metallic CNTs cause higher mobility but reduce the on/off ratio and vice versa. Moreover, in order to increase the sensitivity of carbon nanotubes for bio/chemical sensor application, it is demanded to comprehensively investigate the mechanism for interaction between bio/chemical molecules with the carbon nanotubes surface.

Acknowledgments

Almost four years have passed since I have decided to move to Italy and Germany to achieve my doctorate. To see spectacular views form crystal sea of Amalfi coast to green-land of Weser river, but it was not all my journey; graduate life in different countries can be challenging, particularly as a newcomer. However as time progressed, I gain insight knowledge for what I had always strived for. These challenges have changed me and opened my mind to see different aspects of life that will be valuable experiences for my future life; it is an amazing feeling. I would like to take advantage of this opportunity to thank all people to whom I believe I owe this achievement.

Foremost, I would like to thank my supervisors, dear Prof. Vincenzo Tucci from University of Salerno and dear Prof. Veit Wagner from Jacobs University Bremen, for the wonderful opportunity to join their groups and continue my study as a PhD level, which was one of my dreams. They gave me the chance to study my interesting subject and generously shared with me their expertise and research insight that motivated me to investigate multidisciplinary fields of science. Their thoughtful advices have served to give me sense of motion and direction that helped me to grow even more in my scientific education. I am also thankful for the financial support and the friendly scientific environment in their groups during my PhD. Furthermore, I would like to acknowledge them for correcting and reviewing my thesis.

I would like to special thank dear Prof. Jürgen Fritz as one of my thesis committee members. I am very glad to have him in the committee and I am greatly thankful for his help in reviewing and evaluating my thesis. I would also thank him for the helpful discussions and constructive support about the biological part of this project and for giving me the opportunity to work in his laboratory and set-up my experiments.

I would like to deeply thank dearest Prof. Patrizia Lamberti as one of my thesis committee members. I greatly thank for her constructive idea about the modeling part of my project and her friendly manners throughout my PhD time. I feel she is one of my family members. Thanks again dear Patrizia for spending lots of time, for answering my questions and for motivating me to persist with my study.

I would like to enormously thank dear Prof. Giuseppe Milano from University of Salerno and dear Prof. Danilo Roccatano as a coordinator of this PhD program. I am greatly thankful for this joint program that gave me the opportunity to work in different groups and gain a lot of knowledge from them. In addition, I am also thankful for the financial support in the frame of international PhD program during the time I worked on my project.
I would like to greatly thank Prof. Bill Milne and dear Dr. Matthew Cole from Cambridge University for their valuable suggestion about deposition processes of thin films.
I would like also very thankful dear Dr. Torsten Balster for his valuable support for maintenance of the clean-room, Mr. Frank Rosenkötter for assisting me for plasma-cleaner, Mr. Bernd Von der Kammer for helping for UV-Vis spectroscopy, Ms. Britta Berninghausen and Ms. Sigrid Manns as project assistance, Mr. Peter Tsvetkov and Dr. Svenja Frischholz for their valuable administrative process.
I would like also very thankful dear Eng. Raffaele Raimo and dear Dr. Biago De Vivo as a technician of our laboratory and for their supportive attention for assisting me to solve the bureaucratic problems at University of Salerno and fruitful discussion.
I would also extend my deeply thanks to my dear colleagues and friends of the nanoelectronics laboratory, Dr. Steve Pittner, Dr. Marlis Ortel, Sidhan Bom, Miriam Schwarz, Nivedita Yumnam, Hippolyte Hirwa, Dileep Dhakal and Richa Sharma for their fruitful discussions and for all the nice time spent together. Furthermore, my special thanks Dr. Steve Pittner and Dileep Dhakal for their introduction and information for handling the instruments in the clean-room at the beginning of my studies. I enjoyed all our nice and helpful discussions, and I will look forward to all our future ones.
I would like to thank also dear Dr. Giovanni Spinelli for sharing with me his constructive ideas about the modeling part of the project and for assisting me in developing a numerical algorithm. More than a colleague he has been a true friend.
I would like to sincerely appreciate my dearest friend; Prof. Francesco De Riccardis who spent countless hours proofreading my thesis and also for his useful tips about different views of life. In addition, thank you very much for spending enlightening and memorable time with you and other Italian friends.

I would like also extend my grateful thanks to my dearest Iranian friends, Dr. Mahmood Khabbazi, Dr. Elham Moazami, Eng.Shahab Saneei, Pouyan Alibeigi, Meisam Aghtar, Mehdi Kazemi, Alireza Mazehri Tehrani, Mahdi Ghorbani, Dr.Masih Babaeian, Dr. Navid Afsharipour Faeze Mohaghegh, Sam Ghaseminezhad, Eng.Mehdi Tabatabaei, Morteza Hemmati, Narges Abdali, Dr. Nafiseh Mohammadi, Samaneh Mafakhery, Nasim Rahmani, Samira Khodaei and Dr.Samira Hezaveh. Thank you very much for all of you for sharing unforgettable time and helping me during difficult moments of my life.

I would like also extend my deeply thanks my dearest Italian friends, Dr. Alessandra Braca, Fabio Ottobrino, Gianni Trezza, Dr. Alessandro Giustiniani, Federica Di Meglio, Monica Leonardi, Aldo Scottilo, Katia, Marta, Luca, Antonio, Fave family and De Riccardis family. Thanks a lot for all of you for sharing beautiful and unforgettable time in Italy.

I would like to thank my beloved sisters, Baharak and Safoora, I really appreciate all the help you gave to our parents during the many years when their only son was away.

My biggest thanks go to my beloved parents, Soraya Jeddi and Mohammad Mousavi, to whom this thesis is dedicated. I do remember your excitement and enthusiasm during my study and life. I owe my deep gratitude to my beloved parents whom I can rely on in any situation and who patiently encourage and advise me. I appreciate your immense patience. At the same time, I can imagine the sadness you must have felt at seeing my empty spot at home. My success so far rests on your tireless support.

The list can be endless… I thank all who gave me also a simple smile.

List of Publications

A. Mousavi, P. Lamberti, G. Spinelli, V.Tucci and V.Wagner, "Fabrication and charge transport modeling of thin film transistor based on carbon nanotubes network", IEEE Transactions on Nanotechnology, *Vol:PP, Iss:99, pp x-x, May 2014.* [In reference to IEEE copyrighted material which is used with permission in this thesis, the IEEE does not endorse any of [Jacobs University Bremen and Univeristy of Salerno]'s products or services. Internal or personal use of this material is permitted].

B. Devivo , P.Lamberti, **A. Mousavi,** G. Spinelli, V. Tucci, " On the numerical analysis of EM properties of materials based on carbon nanofiller", *Nanoscience and Nanotechnology conference, Frascati, Rome, Italy, Sep.2013*

A. Mousavi, P. Lamberti, V. Tucci and V. Wagner, "Feasible Industrial Fabrication of Thin Film Transistor based on Randomized Network of Single Walled Carbon Nanotube", *IEEE-ASMC 2013 ,Saratoga, New York, USA, pp. 18-23, May 2013*. [In reference to IEEE copyrighted material which is used with permission in this thesis, the IEEE does not endorse any of [Jacobs University Bremen and Univeristy of Salerno]'s products or services. Internal or personal use of this material is permitted].

A. Mousavi, P. Lamberti, V. Tucci, V. Wagner, "Fabrication of carbon nanotube biosensor for label-free electronic detection of specific protein", *nanomeetsbio workshop, Salerno, Italy, June 2012*

A. Mousavi, P. Lamberti, V. Tucci, V. Wagner, J. Fritz, " solution-based fabrication of thin film transistors with single-walled carbon nanotube" *deutsche physical gesellschaft (DPG) conference, Berlin,Germany March 2012*

A. Mousavi, V. Wagner, P. Lamberti, V. Tucci, "Interdigitated micro-electrode arrays used as biosensors", *deutsche physical gesellschaft (DPG) conference, Dresden, Germany, March 2011*

A. Mousavi, P. Lamberti, V. Tucci, “Tolerance analysis of interdigitated electrode based biosensor with respect to manufacturing parameters uncertainties”, proceeding of , *Applied Sciences in Biomedical and Communication Technologies (ISABEL), 3rd International Symposium, IEEE, Rome, Italy , pp. 1-5, November 2010.* [*In* reference to IEEE copyrighted material which is used with permission in this thesis, the IEEE does not endorse any of [Jacobs University Bremen and Univeristy of Salerno]'s products or services. Internal or personal use of this material is permitted].

References

[1] S. Ijima, "Helical microtubules of graphitic carbon," *Nature*, vol. 354, pp. 56-58, 1991.

[2] S. Iijima and T. Ichihashi, "Single-shell carbon nanotubes of 1-nm diameter," *Nature* vol. 363, pp. 603–605, 1993.

[3] Bethune, Kiang, DeVries, Gorman, Savoy, Vazquez, and Beyers, "The Discovery of Single-Wall Carbon Nanotubes at IBM," *Nature*, vol. 363, pp. 605–607, 1993.

[4] T. D¨urkop, B. M. Kim, and M. S. Fuhrer, "Properties and applications of high-mobility semiconducting nanotubes," *J. Phys.: Condens. Matter*, vol. 16, pp. R553–R580, 2004.

[5] M. S. Dresselhaus, G. Dresselhaus, J. C. Charlier, and E. Hernández, "Electronic, thermal and mechanical properties of carbon nanotubes " *Phil. Trans. R. Soc. Lond.*, vol. 362, pp. 2065–2098, 2004.

[6] J. Bernholc, D. Brenner, M. B. Nardelli, V. Meunier, and C. Roland, "Mechanical and electrical properties of nanotubes " *Annu. Rev. Mater. Res.*, vol. 32, pp. 347–375, 2002.

[7] E. Joselevich, "Electronic Structure and Chemical Reactivity of Carbon Nanotubes: A Chemist's View," *ChemPhysChem*, vol. 5, pp. 619-624, 2004.

[8] A. Thess, R. Lee, P.Nikolaev, H. Dai, P. Petit, J. Robert, C. Xu, Y. Lee, S. Kim, A. Rinzler, D. Colbert, G. Scuseria, D. Tomanek, J. Fischer, and R. Smalley, "Crystalline Ropes of Metallic Carbon Nanotubes," *Science*, vol. 5274, pp. 483-487., 1996.

[9] J. Kong, H. T. Soh, A. M. Cassell, C. F. Quate, and H. Dai, "Synthesis of Individual Single-Walled Carbon Nanotubes on Patterned Silicon Wafers " *Nature*, vol. 395, pp. 878-881, 1998.

[10] A. M. C. J. Kong, and H. Dai, “, "Chemical Vapor Deposition of Methane for Single-Walled Carbon Nanotubes " *Chemical Physics Letters*, vol. 292, pp. 567-574, 1998.

[11] M. Su, B. Zheng, and J. Liu, "A Scalable CVD Method for the Synthesis of Single-Walled Carbon Nanotubes with High

Catalyst Productivity," *Chemical Physics Letters,* vol. 322, pp. 321-326, 2000.

[12] H. M. Cheng, F. Li, G. Su, H. Y. Pan, L. L. He, X. Sun, and M. S. Dresselhaus, "Large-Scale and Low-Cost Synthesis of Single-Walled Carbon Nanotubes by the Catalytic Pyrolysis of Hydrocarbons," *Applied Physics Letters,* vol. 72, pp. 3282-3284, 1998.

[13] P. Nikolaev, M. J. Bronikowski, R. K. Bradley, F. Rohmund, D. T. Colbert, K. A. Smith, and R. E. Smalley, "Gas-Phase Catalytic Growth of Single-Walled Carbon Nanotubes from Carbon Monoxide," *Chemical Physics Letters,* vol. 313, pp. 91-97, 1999.

[14] M. S. Dresselhaus, G. Dresselhaus, and P. Avouris, "Carbon Nanotubes: Synthesis, Structure, Properties, and Applications," ed Berlin: Springer, 2001.

[15] M. Scarselli, P. Castrucci, and M. D. Crescenzi, "Electronic and optoelectronic nano-devices based on carbon nanotubes," *J. Phys.: Condens. Matter,* vol. 24, p. 313202, 2012.

[16] H.-S. P. Wong and D. Akinwande, *Carbon nanotube and graphene device physics* Cambrdige univeristy press, 2011.

[17] H. W. Zhu, C. L. Xu, D. H. Wu, B. Q. Wei, R. Vajtai, and P. M. Ajayan, "Direct Synthesis of Long Single-Walled Carbon Nanotube Strands," *Science,* vol. 296, pp. 884- 886, 2002.

[18] A. Fraczek-Szczypta, E. Menaszek, T. Syeda, A. Misra, M. Alavijeh, J. Adu, and S. Blazewicz, "Effect of MWCNT surface and chemical modification on in vitro cellular response.," *J Nanopart Res.,* vol. 14, pp. 1181 (pp-14), 2012.

[19] S. D. J. Guo, M.S. Lundstrom and M.P. Anantram,, "Towards Multiscale Modeling of Carbon Nanotube Transistors " *International J. on Multiscale Computational Engineering,* vol. 2, pp. 257-276, 2004.

[20] J. Prasek, J. Drbohlavova, J. Chomoucka, J. Hubalek, O. Jasek, V. Adamc, and R. Kizek, "Methods for carbon nanotubes synthesis—review," *J. Mater. Chem,* vol. 21, pp. 15872-15884, 2011.

[21] M. S. Dresselhaus, G. Dresselhaus, and R. Saito, "Physics of carbon nanotubes," *Carbon,* vol. 33, pp. 883–891, 1995.

[22] D. J. Hornbaker, "Electronic structure of carbon nanotube systems measured with scanning tunneling microscopy," PhD,

University of Illinois at Urbana-Champaign, Urbana, Illinois, 2003.
[23] S. Sahoo, "Pressure effects on bond lengths and shape of zigzag single-walled carbon nanotubes," *Indian journal of pure & applied physics*, vol. 49, pp. 367-371, 2011.
[24] P. R. Wallace, "The band theory of graphete," *Phys. Rev. B*, vol. 71, pp. 622–634, 1947.
[25] P. Avouris, Z. Chen, and V. Perebeinos, "Carbon-based electronics," *nature nanotechnology*, vol. 2, pp. 605-515, 2007.
[26] H. Li, C. Xu, N. Srivastava, and K. Banerjee, "Carbon Nanomaterials for Next-Generation interconnects and Passives: Physics, Status and Prospects," *IEEE Trans. on Electron Devices*, vol. 56, pp. 1799-821, 2009.
[27] R. Saito, G. Dresselhaus, and S. Dresselhaus, *Physical Properties of Carbon Nantubes*. London, U. K.: Imperial College Press, 1998.
[28] P. L. McEuen, *Single Wall Carbon Nanotubes*: Physics Word, 2000.
[29] F. Ghaleh, "Characterization of Surface Defects Produced with Focused Ion Beams and Exploration of Applications for Controlled Growth of Nanostructures," Technischen Universität Dortmund, 2008.
[30] R. Saito, *Physical properties of carbon nanotubes*. London: Imperial college press, 2003.
[31] G. W. Hanson, *Fundamentals of Nanoelectronics*: Pearson Prentice Hall, 2008.
[32] E. D. Minot, "Tuning the band structure of carbon nanotubes," PhD, Cornell University USA, 2004.
[33] T. Belin and F. Epron, "Characterization methods of carbon nanotubes: a review," *Materials Science and Engineering: B*, vol. 119, pp. 105-118, 2005.
[34] S. Bandow and S. Asaka, "Effect of the Growth Temperature on the Diameter Distribution and Chirality of Single-Wall Carbon Nanotubes," *Phys. Rev. Lett.*, vol. 80, pp. 3779-3782, 1998.
[35] M. A. Topinka, M. W. Rowe, D. Goldhaber-Gordon, M. D. McGehee, D. S. Hecht, and G. Gruner, "Charge Transport in Interpenetrating Networks of Semiconducting and Metallic Carbon Nanotubes," *Nano Lett.* , vol. 9, pp. 1866-1871, 2009.

[36] A. Turing, "Computing Machinery and Intelligence," *Mind,* vol. 59, pp. 433-460, 1950.
[37] J. Wu, Y.-L. Shen, K. Reinhardt, H. Szu, and B. Dong, "A Nanotechnology Enhancement to Moore's Law," *Applied Computational Intelligence and Soft Computing*, vol. 2013, p. 13 pages, 2013.
[38] J. Knoch, J. Appenzeller, B. Lengeler, R. Martel, P. A. Solomon, Ph. , C. Dieker, K. L. Wang, J. Scholvin, and J. A. del Alamo, "Technology for the fabrication of ultrashort channel metal–oxide–semiconductor field-effect transistors " *Journal of Vacuum Science & Technology* vol. 19, pp. 1737 - 1741 2001.
[39] S. J. Tans, A. R. M. Verschueren, and C. Dekker, "Room-Temperature Transistor Based on a Single Carbon Nanotube," *Nature,* vol. 393, pp. 49-52, 1998.
[40] X. Li, Y. Liu, D. Shi, Y. Sun, G. Yu, and D. Zhu, "Orientational Self-Assembled Field-Effect Transistors Based on a Single-Walled Carbon Nanotube " *Applied Physics Letters*, vol. 87, p. 243102, 2005.
[41] P. A. Alvi, K. M. Lal, M. J. Siddiqui, and A. H. Naqvi, "Cabon nanotube field effect transitors: A review," *Indian journal of pure & applied physics* vol. 43, pp. 899-904, 2005.
[42] A. Javey, J. Guo, D. B. Farmer, Q. Wang, D. Wang, R. G. Gordon, M. Lundstrom, and H. Dai, "Carbon Nanotube Field-Effect Transistors with Integrated Ohmic Contacts and High-K Gate Dielectrics," *Nano Lett.*, vol. 4, pp. 447-450, 2004.
[43] W. Xue, "Nano-assembled carbon nanotube thin film based microstructures, firled effect transitors, and acetylcholine biosensors ", Univeristy of Minnesota, 2007.
[44] H. Klauk, "Organic thin-film transitor," *chem. Soc. Rev.*, vol. 39, pp. 2643-2666, 2010.
[45] S. M. Sze and K.K.Ng, *Physics of Semiconducting Devices*. New York: Wiley, 2007.
[46] C. Wang, J. Zhang, K. Rhu, A. Badmaev, L. G. D. Arco, and C. Zhou, "Wafer-scale fabrication of seprated carbon nanotube thin-film transistors for display applications," *Nano Letters*, vol. 9, pp. 4285-4291, 2009.
[47] K. Xiao, Y. Liu, P. Hu, G. Yu, X. Wang, and D. Zhu, "High-Mobility Thin-Film Transistors Based on Aligned Carbon

Nanotubes " *Applied Physics Letters,* vol. 83, pp. 150-152, 2003.

[48] Q. Cao and J. A. Rogers, "Ultrathin Films of Single-Walled Carbon Nanotubes for Electronics and Sensors: A Review of Fundamental and Applied Aspects," *ADVANCED MATERIALS,* vol. 21, pp. 29-53 2009.

[49] Yan Duan, Jason L. Juhala, Benjamin W. Griffith, and W. Xue, "A comparative analysis of thin-film transistors using aligned and random-network carbon nanotubes," *Journal of Nanoparticle Research,* vol. 15, pp. 1478-8, 2013.

[50] M. Engel, J. P. Small, M. Steiner, M. Freitag, A. A. Green, M. C. Hersam, and P. Avouris, "Thin film nanotube transistors based on self-Assembled, aligned,semiconducting carbon nanotube Arrays," *ACS Nano,* vol. 2, pp. 2445-2452, 2008.

[51] S.-H. Hur, D.-Y. Khang, C. Kocabas, and J. A. Rogers, "Nanotransfer Printing by Use of Noncovalent Surface Forces: Applications to Thin-Film Transistors That Use Single-Walled Carbon Nanotube Networks and semiconducting Polymers," *Applied Physics Letters,* vol. 85, pp. 5730-5732, 2004.

[52] S.-H. Hur, M.-H. Yoon, A. Gaur, M. Shim, A. Facchetti, T. J. Marks, and J. A. Rogers, "Organic Nanodielectrics for Low Voltage Carbon Nanotube Thin Film Transistors and Complementary Logic Gates," *Journal of the American Chemical Society,,* vol. 127, pp. 13807-13808, 2005.

[53] C. Wang, J. Zhang, K. Ryu, A. Badmaev, L. G. D. Arco, and C. Zhou, "Wafer-scale fabrication of seprated carbon nanotube thin film transistors for dispaly applications," *Nano Letters,* vol. 9, pp. 4285-4291, 2009.

[54] N. Rouhi, D. Jain, K. Zand, and P. J. Burke, "Fundamental Limits on the Mobility of Nanotube-Based Semiconducting Inks," *Advanced Materials,* vol. 23, pp. 94-99, 2011.

[55] R. Chris, Dheeraj, and P. Burke, "Nanotube electronics for radiofrequency applications," *Nature Nanotechnology,* vol. 4, pp. 811-819, 2009.

[56] Q. Cao and J. A. Rogers, "Random Networks and Aligned Arrays of Single-Walled Carbon Nanotubes for Electronic Device Applications," *Nano Res.,* vol. 1, p. 259 272, 2008.

[57] E. S. Snow, P. M. Campbell, M. G. Ancona, and J. P. Novak, "High-Mobility Carbon-Nanotube Thin-Film Transistors on a

Polymeric Substrate " *Applied Physics Letters,* vol. 86, pp. 033105-3, 2005.

[58] Q. Fu, S. Huang, and J. Liu, "Chemical Vapor Depositions of Single-Walled Carbon Nanotubes Catalyzed by Uniform Fe2O3 Nanoclusters Synthesized Using Diblock Copolymer Micelles," *J. Phys. Chem. B,* vol. 108, pp. 6124-6129, 2004.

[59] O. Matarredona, H. Rhoads, Z. Li, J. H. Harwell, L. Balzano, and D. E. Resasco, "Dispersion of Single-Walled Carbon Nanotubes in Aqueous Solutions of the Anionic Surfactant NaDDBS," *J. Phys. Chem. B,* vol. 107, pp. 13357-13367, 2003.

[60] Q. Cao and J. A. Rogers, "Ultrathin Films of Single-Walled Carbon Nanotubes for Electronics and Sensors: A Review of Fundamental and Applied Aspects," *Advanced Materials,* vol. 21, pp. 29-53, 2008.

[61] D. Jain, N. Rouhi, C. Rutherglen, C. G. Densmore, S. K. Doorn, and P. J. Burke, "Effect of Source, Surfactant, and Deposition Process on Electronic Properties of Nanotube Arrays," *Journal of Nanomaterials* vol. 2011, pp. 1-7, 2010.

[62] B. R. Baker, R. Y. Lai, M. S. Wood, E. H. Doctor, A. J. Heeger, and K. W. Plaxco, "An Electronic, Aptamer-Based Small-Molecule Sensor for the Rapid, Label-Free Detection of Cocaine in Adulterated Samples and Biological Fluids " *Am. Chem. Soc.,* vol. 128, pp. 3138–3139, 2006.

[63] S. N. Kim, J. F. Rusling, and F. Papadimitrakopoulos, "Carbon Nanotubes for Electronic and Electrochemical Detection of Biomolecules," *Advanced Materials,* vol. 19, pp. 3214–3228, 2007.

[64] X. Yang, Y. Lu, Y. Ma, Z. Liu, F. Du, and Y. Chen, "DNA electrochemical sensor based on an adduct of single-walled carbon nanotubes and ferrocene," *Biotechnol Lett* vol. 29, pp. 1775–1779, 2007.

[65] J. Zhao, A. Buldum, J. Han, and J. P. Lu, "Gas molecule adsorption in carbon nanotubes and nanotube bundles " *Nanotechnology,* vol. 13, pp. 195-200, 2002.

[66] Y. Wang, Z. Tang, and N. A. Kotov, "Bioapplication of nanosemiconductors," *Nanotoday,* vol. 8, pp. 20-31, 2005.

[67] J. Wang, "Carbon-Nanotube Based Electrochemical Biosensors: A Review," *Electroanalysis,* vol. 17, pp. 7-14, 2005.
[68] A. C. Dillon, K. M. Jones, T. A. Bekkedahl, C. H. Kiang, D. S. Bethune, and M. J. Heben, "Storage of hydrogen in single-walled carbon nanotubes," *Nature,* vol. 386, pp. 377-379, 1997.
[69] R. Lalauze, *Chemical sensors and biosensors*. USA: Wiley, 2012.
[70] P. Hu, A. Fasoli, J. Park, Y. Choi, P. Estrela, S. L. Maeng, W. I. Milne, and A. C. Ferrari, "Self-assembled nanotube field-effect transistors for label-free protein biosensors," *JOURNAL OF APPLIED PHYSICS,* vol. 104, pp. 743101-743105, 2008.
[71] Z. Xu, X. Chen, X. Qu, J. Jia, and S. Dong, "Single-Wall Carbon Nanotube-Based Voltammetric Sensor and Biosensor " *Biosensors and Bioelectronics,* vol. 20, pp. 579-584, 2004.
[72] M. Zheng, A. Jagota, E. D. Semke, B. A. Diner, R. S. Mclean, S. R. Lustig, R. E. Richardson, and N. G. Tassi, "DNA-assisted dispersion and separation of carbon nanotubes," *Nature Materials* vol. 2, pp. 338 - 342, 2003.
[73] K. Bradley, M. Briman, A. Star, and G. Grüner, "Charge Transfer from Adsorbed Proteins," *Nano Lett.,* vol. 4, pp. 253-256, 2004.
[74] N. V. Pimparkar, S. Kumar, J. Y. Murthy, and M. A. Alam, "Current-Voltage Characteristics of Long- Channel Nanobundle Thin-Film Transistors: A 'Bottom-up' Perspective," *Electron Device Letters, IEEE,* vol. 28, pp. 157-160, 2007.
[75] A. Behnam, G. Bosman, and A. Ural, "Percolation scaling of 1/f noise in single-walled carbon nanotube films. ,:," *Phys. Rev. B,* vol. 78, pp. 085431-085439, 2008.
[76] Y.Zhang, A. Chang, J. Cao, Q. Wang, W. Kim, Y. Li, N. Morris, E. Yenilmez, J.Kong, and H. Dai, "Electric-field-directed growth of aligned single-walled carbon nanotubes " *Appl. Phys. Lett. ,* vol. 79, pp. 3155-3157, 2001.
[77] M. M. A. Rafique and J. Iqbal, "Production of Carbon Nanotubes by Different Routes— A Review," *Journal of Encapsulation and Adsorption Sciences,* vol. 1 pp. 29-34, 2011.

[78] X. Li, L. Zhang, X. Wang, I. Shimoyama, X. Sun, W.-S. Seo, and H. Dai, "Langmuir−Blodgett Assembly of Densely Aligned Single-Walled Carbon Nanotubes from Bulk Materials," *J. Am. Chem. Soc.*, vol. 129, pp. 4890-4891, 2007.
[79] V. N. Popov, "Carbon nanotubes: properties and application," *Materials Science and Engineering,* vol. 43, pp. 61-102, 2004.
[80] Loiseau, Launois-Bernede, Petit, Roche, and Salvetat, *Understanding carbon nanotubes : from basics to applications* Berlin Springer, 2006.
[81] H. J. Dai, "Carbon nanotubes: Synthesis, integration, and properties," *Accounts of Chemical Research,* vol. 35, pp. 1035-1044, 2002.
[82] S. Yellampalli, *carbon nanotubes- synthesis, characterization, application* InTech, 2011.
[83] G. Che, B. B. Lakshmi, C. R. Martin, E. R. Fisher, and R. S. Ruoff, "Chemical vapor deposition based synthesis of carbon nanotubes and nanofibers using a template method," *Chemistry of Materials,* vol. 10, pp. 260-267, 1998.
[84] H. Hafner, M. J. Bronikowski, B. R. Azamian, P. Nikolaev, A. G. Rinzler, D. T. Colbert, K. A. Smith, and R. E. Smalley, "Catalytic growth of single-wall carbon nanotubes from metal particles " *Chemical Physics Letters,* vol. 296, pp. 195-202, 1998.
[85] M. C. Hersam, "Progress towards monodisperse single-walled carbon nanotubes," *Nature Nanotechnology,* vol. 3, pp. 387-394, 2008.
[86] R. Krupke and F. Hennrich, "Separation techniques for carbon nanotubes " *Adv. Engineer. Mat.*, vol. 7, pp. 111–116 2005.
[87] Banerjee, Hemraj-Benny, and Wong, "Routes towards separating metallic and semiconducting nanotubes," *J. Nanosci. Nanotechnol,* vol. 5, pp. 841–855, 2005.
[88] C. Kocabas, N. Pimparkar, O. Yesilyurt, S. J. Kang, M. A. Alam, and J. A. Rogers, "Experimental and Theoretical Studies of Transport through Large Scale, Partially Aligned Arrays of Single-Walled Carbon Nanotubes in Thin Film Type Transistors," *Nano Letters,* vol. 7, pp. 1195-1202, 2007.
[89] H. Choi, J. Gong, Y. Lim, K. H. Im, and M. Jeon, "Effects of the electrical conductivity and orientation of silicon substrate on the synthesis of multi-walled carbon nanotubes by thermal

chemical vapor deposition," *nano reserach letters* vol. 8, p. 110, 2013.

[90] D. Jain, N. Rouhi, C. Rutherglen, C. G. Densmore, S. K. Doorn, and P. J. Burke, "Effect of Source, Surfactant, and Deposition Process on Electronic Properties of Nanotube Arrays," *Journal of Nanomaterials,* vol. 2011, pp. 1-7, 2011.

[91] R. Anderson and A. Barron, "Solubilization of single-wall carbon nanotubes in Organic solvents without sidewall functionalization," *J Nanosci Nanotechnol,* vol. 10, pp. 3436-40, 2007.

[92] S. Manivannan, O. Jeong, J. H. Ryu, C. S. Lee, K. S. Kim, J. Jang, and K. C. Park, "Dispersion of single-walled carbon nanotubes in aqueous and organic solvents through a polymer wrappingfunctionalization," *J Mater Sci: Mater Electron* vol. 20, pp. 223–229, 2009.

[93] G. W. Lee and S. Kumar, "Dispersion of nitric acid-treated SWNTs in organic solvents and solvent mixtures," *Journal of Physical Chemistry B,* vol. 109, pp. 17128-17133, 2005.

[94] L. Vaisman, H. D. Wagner, and G. Marom, "The role of surfactants in dispersion of carbon nanotubes," *Advances in Colloid and Interface Science,* vol. 128, pp. 37-46,, 2006.

[95] H. J. Huang, H. Kajiura, A. Yamada, and M. Ata, "Purification and alignment of arc-synthesis single-walled carbon nanotube bundles," *Chemical Physics Letters,* vol. 356, pp. 567-572, 2002.

[96] H. Hu, B. Zhao, M. E. Itkis, and R. C. Haddon, "Nitric Acid Purification of Single-Walled Carbon Nanotubes," *Journal of Physical Chemistry,* vol. 107, pp. 13838-13842, 2003.

[97] H. Wang, "Dispersing carbon nanotubes using surfactants," *Current Opinion in Colloid & Interface Science,* vol. 14, pp. 364–371, 2009.

[98] J. Chen, A. M. Rao, S. Lyuksyutov, M. E. Itkis, M. A. Hamon, H. Hu, R. W. Cohn, P. C. Eklund, D. T. Colbert, R. E. Smalley, and R. C. Haddon, "Dissolution of Full-Length Single-Walled Carbon Nanotubes," *J. Phys. Chem. B* vol. 105, pp. 2525-2528, 2001.

[99] M. N. Tchoul, W. T. Ford, G. Lolli, D. E. Resasco, and S. Arepalli, "Effect of Mild Nitric Acid Oxidation on Dispersability, Size, and Structure of Single- Walled Carbon

Nanotubes " *Chemistry of Materials*, vol. 19, pp. 5765-5772, 2007.

[100] R. K. Jackson, "Development of single wall carbon nanotube transparent conductive electrodes for organic electronics," Georgia Institute of Technology, 2009.

[101] S. Qin, D. Qin, W. T. Ford, D. E. Resasco, and J. E. Herrera, "Polymer Brushes on Single-Walled Carbon Nanotubes by Atom Transfer Radical Polymerization of n-Butyl Methacrylate," *AM. CHEM. SOC.*, vol. 126, pp. 170-176, 2004.

[102] Y. Q. Tan and D. E. Resasco, "Dispersion of single-walled carbon nanotubes of narrow diameter distribution," *Journal of Physical Chemistry*, vol. 109, pp. 14454-14460, 2005.

[103] D. Zhang, K. Ryu, X. Liu, E. Polikarpov, J. Ly, M. E. Tompson, and C. Zhou, "Transparent, conductive, and flexible carbon nanotube films and their application in organic light-emitting diodes," *Nano Letters*, vol. 6, pp. 1880-1886, 2006.

[104] Z. H. C. Z. C. Wu, X. Du, J. M. Logan, J. Sippel, M. Nikolou, K. Kamaras, J. and D. B. T. R. Reynolds, A. F. Hebard, and A. G. Rinzler, " "Transparent conductive carbon nanotube films," *Science*, vol. 305, pp. 1273-1276, 2004.

[105] W. H. Duan, Q. Wang, and F. Collinsa, "Dispersion of carbon nanotubes with SDS surfactants: a study from a binding energy perspective " *Chem. Sci.*, vol. 2, pp. 1407-1413, 2011.

[106] V. C. Moore, M. S. Strano, E. H. Haroz, R. H. Hauge, R. E. Smalley, J. Schmidt, and Y. Talmon, "Individually Suspended Single-Walled Carbon Nanotubes in Various Surfactants," *Nano Letters*, vol. 3, pp. 1379-1382, 2003.

[107] Y. Tian, B. Gao, and K. Ziegler, "High mobility of SDBS-dispersed single-walled carbon nanotubes in saturated and unsaturated porous media," *J Hazard Mater.*, vol. 186, pp. 2-3, 2011.

[108] Y. Bai, D. Lin, F. Wu, Z. Wang, and B. Xing, "Adsorption of Triton X-series surfactants and its role in stabilizing multi-walled carbon nanotube suspensions," *Chemosphere*, vol. 79, pp. 362-367, 2010.

[109] M. H. A. Ng, L. T. Hartadi, T. Huiwen, and C. H. P. Poa, "Efficient coating of transparent and conductive carbon

nanotube thin films on plastic substrates," *Nanotechnology,* vol. 19, pp. 205703-8, 2008.
[110] M. r. D. Lima, M. n. J. d. Andrade, C. P. Bergmannb, and S. Rotha, "Thin, conductive, carbon nanotube networks over transparent substrates by electrophoretic deposition," *J. Mater. Chem.,* vol. 18, pp. 776-779, 2008.
[111] L. Filipovic, "Topography Simulation of Novel Processing Technique," Technischen Universität Wien 2012.
[112] M. Jeong, K. Lee, E. Choi, A. Kim, and S.-B. Lee, "Spray-coated carbon nanotube thin-film transistors with striped transport channels," *Nanotechnology,* vol. 23, p. 505203 (5pp), 2012.
[113] M. H. A. Ng, L. T. Hartadi, T. Huiwen, and C. H. P. Poa, "Efficient coating of transparent and conductive carbon nanotube thin films on plastic substrates," *Nanotechnology,* vol. 19, p. 205703 (5 pp.), 2008.
[114] X. Xiong, C.-L. Chen, P. Ryan, A. A. Busnaina, Y. J. Jung, and M. R. Dokmeci, "Directed assembly of high density single-walled carbon nanotube patterns on flexible polymer substrates," *Nanotechnology,* vol. 20, p. 295302 (6pp), 2009.
[115] P. M. Martin, *Handbook of Deposition Technologies for Films and Coatings*: Elsevier Inc., 2010.
[116] M. A. Meitl, Y. Zhou, A. Gaur, S. Jeon, M. L. Usrey, M. S. Strano, and J. A. Rogers, "Solution Casting and Transfer Printing Single-Walled Carbon Nanotube Films," *NANO LETTERS,* vol. 4, pp. 1643-1647
2004.
[117] M. C. LeMieux, M. Roberts, S. Barman, Y. W. Jin, J. M. Kim, and Z. Bao, "Self-Sorted, Aligned Nanotube Networks for Thin-Film Transistors," *Science,* vol. 321 pp. 101-104, 2008.
[118] M. C. LeMieux, S. Sok, M. E. Roberts, J. P. Opatkiewicz, D. Liu, S. N. Barman, N. Patil, S. Mitra, and Z. Bao, "Solution Assembly of Organized Carbon Nanotube Networks for Thin-Film Transistors," *ACS Nano,* vol. 3, pp. 4089-4097, 2009.
[119] S. Williams, "Dielectrophoretic Motion of Particles and Cells," in *Encyclopedia of Microfluidics and Nanofluidics* ed: Springer, 2008, pp. 357-364

[120] J. Li, Q. Zhang, D. Yang, and J. Tian, "Fabrication of carbon nanotube field effect transistors by AC dielectrophoresis method," *Carbon*, vol. 42, pp. 2263–2267, 2004.

[121] S. Shekhar, P. Stokes, and S. I. Khondaker, "Ultrahigh Density Alignment of Carbon Nanotube Arrays by Dielectrophoresis," *ACS Nano*, vol. 5, pp. 1739-1746 2011.

[122] L. Nagahara, I. Amlani, J. Lewenstein, and R. Tsui, " Directed placement of suspended carbon nanotubes for nanometer-scaleassembly," *Appl Phys Lett* vol. 80, pp. 3826–8, 2002.

[123] Krupke, Hennrich, Weber, Kapper, and Lohneysen, "Simultaneous deposition of metallic bundles of single-walled carbon nanotubes using Ac-dielectrophoresis " *Nano Lett.*, vol. 3, pp. 1019–23, 2003.

[124] http://www.sigmaaldrich.com/catalog/product/aldrich/704148?lang=en&region=RO. (2013). *90% semiconducting single walled carbon nanotube*.

[125] B. R. Priya and H. J. Byrne, "Investigation of Sodium Dodecyl Benzene Sulfonate Assisted Dispersion and Debundling of Single-Wall Carbon Nanotubes " *J. Phys. Chem.*, vol. 112, pp. 332–337, 2008.

[126] M. S. ARNOLD, A. A. GREEN, J. F. HULVAT, S. I. STUPP, and M. C. HERSAM, "Sorting carbon nanotubes by electronic structure using density differentiation," *nature nanotechnology*, vol. 1, pp. 60-65, 2006.

[127] J. Wu, L. Jiao, A. Antaris, C. L. Choi, L. Xie, Y. Wu, S. Diao, C. Chen, Y. Chen, and H. Dai, "Self-Assembly of Semiconducting Single-Walled Carbon Nanotubes into Dense and Aligned Rafts," *small*, pp. 1-28, 2013.

[128] D. Chattopadhyay, I. Galeska, and F. Papadimitrakopoulos, "A Route for Bulk Separation of Semiconducting from Metallic Single-Wall Carbon Nanotubes," *J. Am. Chem. Soc.*, vol. 125, pp. 3370–3375, 2003.

[129] Y. Zhao and W. Li, "Fluctuation-induced tunneling dominated electrical transport in multi-layered single-walled carbon nanotube films," *Thin solid films*, vol. 519, pp. 7987-7991, 2011.

[130] L. Hu, D. S. Hecht, and G. Groner, "Percolation in Transparent and Conducting Carbon Nanotube Networks," *Nano Letters*, vol. 4, pp. 2513-2517, 2004.
[131] A. Mousavi, P. Lamberti, and V. Tucci, "Tolerance analysis of interdigitated electrode based biosensor with respect to manufacturing parameters uncertainties " in *Applied Sciences in Biomedical and Communication Technologies (ISABEL), 2010 3rd International Symposium on* 2010, pp. 1 -5.
[132] Sedra/Smith, *Microelectronic circuits*. New York Oxford: OXFORD UNIVERSITY PRESS, 2004.
[133] C. RoyChaudhuri and R. D. Das, "A biomolecule compatible electrical model of microimpedance affinity biosensor for sensitivity improvement in cell detection," *Sensors and Actuators A: Physical*, vol. 157, pp. 280-289, 2010.
[134] X. Xian, W. Z. Kai Yan, L. Jiao, ZhongyunWu, and Z. Liu, "Unipolar p-type single-walled carbon nanotube field-effect transistors using TTF–TCNQ as the contact material
" *Nanotechnology (2009) 505204 (5pp)*, vol. 20, pp. 1-5, 2009.
[135] P. L. McEuen, M. S. Fuhrer, and H. Park, "Single-Walled Carbon Nanotube Electronics," *IEEE TRANSACTIONS ON NANOTECHNOLOGY*, vol. 1, pp. 78-85, 2002.
[136] NanoIntegris-Inc. (2012). *Technical specification data sheet of semiconducting SWNTs*. Available: http://www.nanointegris.com/en/semiconducting. .
[137] N. Rouhi, D. Jain, and P. J. Burke, "High-Performance Semiconducting Nanotube Inks: Progress and Prospects," *ACS Nano*, vol. 5, pp. 8471–8487, 2011.
[138] C.-H. Chung, T.-B. Song, B. Bob, R. Zhu, and Y. Yang, "Solution-Processed Flexible Transparent Conductors Composed of Silver Nanowire Networks Embedded in Indium Tin Oxide Nanoparticle Matrices," *Nano reserach letters*, vol. 5, pp. 805-814, 2012.
[139] Q. Cao, M. Xia, C. Kocabas, M. Shim, J. Roger, and S. Rotkin, "Gate capacitance coupling of singled-walled carbon nanotube thin-film transistors," *Appl. Phys Lett*, vol. 90, pp. 0235161-0235163, 2007.
[140] D.-m. Sun, M. Y. Timmermans, Y. Tian, A. G. Nasibulin, E. I. Kauppinen, S. Kishimoto, T. Mizutani, and Y. Ohno, "Flexible

high-performance carbon nanotube integrated circuits," *Nature Nanotechnology*, vol. 6, pp. 156–161, 2011.

[141] S. Rosenblatt, Y. Yaish, J. Park, J. Gore, V. Sazonova, and P. L. McEuen:, "High Performance Electrolyte Gated Carbon Nanotube Transistors," *Nano Lett.*, vol. 2, pp. 869-872, 2002.

[142] P. Sonar, S. P. Singh, Y. Li, Z.-E. Ooi, T.-j. Ha, I. Wong, M. S. Soh, and a. A. Dodabalapur, "High mobility organic thin film transistor and efficient photovoltaic devices using versatile donor–acceptor polymer semiconductor by molecular design. ," *Energy Environ. Sci.*, vol. 4, pp. 2288-2296, 2011.

[143] B. Stannowski, R. E. I. Schropp, R. B. Wehrspohn, and M. J. Powell, "Amorphous-silicon thin-film transistors deposited by VHF-PECVD and hot-wire CVD," *Non-Cryst. Solids* , , vol. 1340, pp. 299–302, 2002.

[144] Zhou, X. Park, J.-Y. Huang, Shaoming, J. Liu, and P. L. McEuen, "Band Structure, Phonon Scattering, and the Performance Limit of Single-Walled Carbon Nanotube Transistors," *Physical Review Letters*, vol. 95, pp. 1468051-4, 2005.

[145] S. Kumar, N. Pimparkar, J. Y. Murthy, and M. A. Alam, "Theory of transfer characteristics of nanotube network transistors," *Applied Physics Letters*, vol. 88, pp. 1235051-3, 2006.

[146] M. S. Fuhrer, J. Nyg rd, L. Shih, M. Forero, Y.-G. Yoon, M. S. C. Mazzoni, H. J. Choi, J. Ihm, S. G. Louie, A. Zettl, and P. L. McEuen, "Crossed Nanotube Junctions," *SCIENCE*, vol. 288, pp. 494-497, 2000.

[147] C. Wang, J. Zhang, and C. Zhou, "Macroelectronic Integrated Circuits Using High-Performance Separated Carbon Nanotube Thin-Film Transistors," *ACS Nano*, vol. 4, pp. 7123–7132, 2010.

[148] F. C. H. Tam, T. K. W. Ling, K. T. Wong, D. T. M. Leung, R. C. Y. Chan, and P. L. Lim, "The TUBEX test detects not only typhoid-specific antibodies but also soluble antigens and whole bacteria " *J. Med. Microbiol*, vol. 57, pp. 316–323, 2008.

[149] Niemeyer and C. M., "Nanoparticles, proteins, and nucleic acids: biotechnology meets materials science," *Chem. Int. Ed*, vol. 40, pp. 4128-4158, 2001.

[150] G. Spinelli, A. Giustiniani, P. Lamberti, V. Tucci, and W. Zombani, "Numerical study of electrical behaviour in carbon nanotube composit," *Int. J. Appl. Electron,* vol. 39, pp. 21-27, 2012.
[151] B. D. Vivo, P. Lamberti, G. Spinelli, and V. Tucci, "Numerical investigation on the influence factors of the electrical properties of catbon nanotubes-filled composites," *JOURNAL OF APPLIED PHYSICS,* vol. 113, p. 244301, 2013.
[152] A. Mousavi, P. Lamberti, V. Tucci, and V. Wagner, "Feasible industrial fabrication of thin film transistor based on randomized network of single walled carbon nanotubes " in *IEEE-Advanced Semiconductor Manufacturing Conference (ASMC), 2013 24th Annual SEMI* 2010, pp. 18-23.
[153] G. E. Pike and C. H. Seager, "Percolation and Conductivity: A computer study," *Physical Review B,* vol. 10, pp. 1421-1434, 1974.
[154] C. Kocabas, N. Pimparkar, O. Yesilyurt, S. J. Kang, M. A. Alam, and J. A. Rogers, "Experimental and Theoretical Studies of Transport through Large Scale, Partially Aligned Arrays of Single-Walled Carbon Nanotubes in Thin Film Type Transistors," *Nano Letters,* vol. 7, pp. 1195-1202, 2007.
[155] F. Kreupl and Q. AG, *Carbon Nanotubes devices*: Wiley, 2008.
[156] J. H. Simmons, "Generalized Formula for the Electric Tunnel Effect between Similar Electrodes Separated by a Thin Insulating Film," *J. Appl. Phys,* vol. 34, pp. 1793-1803, 1963.
[157] C. Li, E. T. Thostenson, and T.-W. Chou, "Dominant role of tunnelling resistance in the electrical conductivity of carbon nanotube-based composites," *Appl. Phys. Lett.* , vol. 91, pp. 223114-7, 2007.
[158] F. Du, J. E. Fischer, and K. I. Winey, "Effect of nanotube alignment on percolation conductivity in carbon nanotube/polymer composites," *Physical Review B,* vol. 72, pp. 1214041-4, 2005.
[159] J. W. G. Wildo, L. C. Venema, A. G. Rinzler, R. E. Smalley, and C. Dekker, "Electronic structure of atomically resolved carbon nanotubes," *Nature* vol. 391, pp. 59-62, 1998.
[160] M. Garretta, I. N. Ivanova, D. Geohegana, and B. Huc, "Effect of purity on the electro-optical properties of single wall

nanotube-based transparent conductive electrodes," *Carbon,* vol. 64, pp. 1-5, 2013.

[161] E. Bekyarova, M. E. Itkis, N. Cabrera, B. Zhao, A. Yu, J. Gao, and R. C. Haddon, "Electronic Properties of Single-Walled Carbon Nanotube Networks," *Journal of the American Chemical Society*, vol. 127, pp. 5990–5995, 2005.

[162] C. Wang, J. Zhang, K. Ryu, A. Badmaev, L. G. D. Arco, and C. Zhou, "Wafer-scale fabrication of seprated carbon nanotube thin film transistors for dispaly applications," *Nano Letters*, vol. 9, pp. 4285-4291, 2009.

[163] B. N. G. Giepmans, S. R. Adams, M. H. Ellisman, and R. Y. Tsien, "The Fluorescent Toolbox for Assessing Protein Location and Function," *Science*, vol. 312, pp. 217-224, 2006.

[164] C. J. Weijer, "Visualizing Signals Moving in Cells," *Science*, vol. 300 pp. 96-100 2003.

[165] P. Hu, J. Zhang, L. Li, Z. Wang, W. O'Neill, and P. Estrela, "Carbon Nanostructure-Based Field-Effect Transistors for Label-Free Chemical/Biological Sensors," *Sensors* vol. 10, pp. 5133-5159, 2010.

[166] C. Huang and H.-T. Chang, "Selective Gold-Nanoparticle-Based "Turn-On" Fluorescent Sensors for Detection of Mercury(II) in Aqueous Solution," *Anal. Chem.,* vol. 78, pp. 8332–8338, 2006.

[167] J. K. Herr, J. E. Smith, C. D. Medley, D. Shangguan, and W. Tan, "Aptamer-Conjugated Nanoparticles for Selective Collection and Detection of Cancer Cells," *Anal. Chem.,* vol. 78, pp. 2918–2924, 2006.

[168] X.-N. Wang and P.-A. Hu, "Carbon nanomaterials: controlled growth and field-effect transistor biosensors," *Frontiers of Materials Science*, vol. 6, pp. 26-46, 2012.

[169] O. Lazcka, F. J. D. Campob, and F. X. Mu˜noz, "Pathogen detection: A perspective of traditional methods and biosensors" Biosensors and Bioelectronics," *Biosensors and Bioelectronics,* vol. 22, pp. 1205–1217, 2007.

[170] P. Belgrader, W. Benett, D. Hadley, G. Long, R. Marialla, F. Milanovich, S. Nasarabadi, W. Nelson, J. Richards, and P. Stratton, "Rapid pathogen detection using a microchip PCR array instrument," *Clin. Chem*, vol. 44, pp. 2191–2194, 1998.

[171] H. Wei, B. Li, J. Li, E. Wang, and S. Dong, "Simple and sensitive aptamer-based colorimetric sensing of protein using unmodified gold nanoparticle probes," *Chem.comm*, pp. 3735–3737, 2007.
[172] L. J, S. CM, M. BL, and R. LJ, "Reflective interferometric detection of label-free oligonucleotides," *Anal. Chem.*, vol. 76, pp. 4416-4420, 2004.
[173] G. Zheng, F. Patolsky, Y. Cui, W. U. Wang, and C. M. Lieber, "Multiplexed electrical detection of cancer markers with nanowire sensor arrays," *Nature Biotechnology*, vol. 23, pp. 1294 - 1301, 2005.
[174] A. Star, E. Tu, J. Niemann, Jean-Christophe P. Gabriel, C. S. Joiner, and C. Valcke, "Label-free detection of DNA hybridization using carbon nanotube network field-effect transistors," *Proc.Natl.Acad.Sci. USA*, vol. 103, pp. 921-926, 2006.
[175] Z. Liu, F. Galli, K. G. H. Janssen, L. Jiang, H. J. V. d. Linden, D. C. d. Geus, and j. P. Abrahams, "Stable single-walled carbon nanotube-streptavidin complex for biorecognition," *J. Phys. Chem. C*, vol. 114, pp. 4345-4352, 2010.
[176] T. Durkop, S. A. Getty, E. Cobas, and M. S. Fuhrer, "Extraordinary Mobility in Semiconducting Carbon Nanotubes," *Nano Letters*, vol. 4, pp. 35-39 2004.
[177] K. Dasgupta, S. Kar, R. Venugopalan, R. C. Bindal, S. Prabhakar, P. K. Tewari, S. Bhattacharya, S. K. Gupta, and D. Sathiyamoorthy, "Self-standing geometry of aligned carbon nanotubes with high surface area," *Materials Letter*, vol. 62, pp. 1989–1992, 2008.
[178] G. Gruner, "Carbon nanotube transistors for biosensing applications," *Analytical and bioanalytical chemistry*, vol. 384,, pp. 322–335, 2006.
[179] I. Heller, A. M. Janssens, J. Mannik, E. D. Minot, S. G. Lemay, and C. Dekker, "Identifying the Mechanism of Biosensing with Carbon Nanotube Transistors," *Nano Letters*, vol. 8, pp. 591-595, 2008.
[180] A. Maroto, K. Balasubramanian, M. Burghard, and K. Kern, "Functionalized Metallic Carbon Nanotube Devices for pH Sensing," *ChemPhysChem*, vol. 8, pp. 220 – 223, 2007.

[181] R. Martel, T. Schmidt, H. R. Shea, T. Hertel, and P. Avouris, "Single- and multi-wall carbon nanotube field effect transistors," *APPLIED PHYSICS LETTERS,* vol. 73, pp. 2447-2449, 1998.

[182] M. Mattmann, T. Helbling, L. Durrer, C. Roman, C. Hierold, R. Pohle, and M. Fleischer, "Sub-ppm NO_2 detection by Al_2O_3 contact passivated carbon nanotube field effect transistors " *Appl. Phys. Lett.,* vol. 94, pp. 1835021-3, 2009.

[183] J. Suehiro, G. Zhou, and M. Hara, "Detection of partial discharge in SF_6 gas using a carbon nanotube-based gas sensor," *Sens. Actuators B,* vol. 105, pp. 164-169, 2005.

[184] E. L. Gui, L.-J. Li, K. Zhang, Y. Xu, X. Dong, X. Ho, P. S. Lee, J. Kasim, Z. X. Shen, J. A. Rogers, and S.G, "DNA Sensing by Field-Effect Transistors Based on Networks of Carbon Nanotubes," *J. Am. Chem. Soc.,* vol. 129, pp. 14427–14432, 2007.

[185] P. Hu, A. Fasoli, J. Park, Y. Chio, and P. Estrela, "Self-assembled nanotube field-effect transistors for label-free protein biosensors," *J. Appl. Phys,* vol. 104, pp. 0743101-5, 2008.

[186] A. star, J.-C. P. Gabriel, K. Bradley, and G. Gruner, "Electronic detection of specific protein binding using nanotube FET devices," *Nano Letters,* vol. 3, pp. 459-463, 2003.

[187] F. Balavoine, P. Schultz, Cyrille Richard1, V. Mallouh, T. W. Ebbesen, and C. Mioskowski, "Helical crystallization of proteins on carbon nanotubes: a first step towards the development of new biosensors," *Angew. Chem. Int. Ed.,* vol. 38, pp. 1912–1915, 1999.

[188] N. W. S. Kam and H. Dai, "Carbon Nanotubes as Intracellular Protein Transporters: Generality and Biological Functionality," *J. Am. Chem.,* vol. 127, pp. 6021–6026, 2005.

[189] S. Niyogi, M. A. Hamon, H. Hu, B.Zhao, P.Bhowmik, R. Sen, M. E. Itkis, and R. C. Haddon, "Chemistry of single-walled carbon nanotubes," *Acc. Chem. Res,* vol. 35, pp. 1105–1113, 2002.

[190] R. J. Chen, Y. Zhang, D. Wang, and H. Dai, "Noncovalent sidewall functionalization of singlewalled carbon nanotubes

for protein immobilization.," *J. Am. Chem. Soc.*, vol. 123, pp. 3838–3839, 2001.

[191] S.Sotiropoulou and N. Chaniotakis, "Carbon nanotube array-based biosensor," *Anal. Bioanal. Chem*, vol. 375, pp. 103-105, 2003.

[192] H. R. Byon and H. C. Choi, "Network Single-Walled Carbon Nanotube-Field Effect Transistors (SWNT-FETs) with Increased Schottky Contact Area for Highly Sensitive Biosensor Applications," *J. Am. Chem. Soc.*, vol. 128, pp. 2188–2189, 2006.

[193] R. J. Chen, S. Bangsaruntip, K. A. Drouvalakis, N. W. S. Kam, M. Shim, Y. Li, W. Kim, P. J. Utz, and H. Dai, "Noncovalent functionalization of carbon nanotubes for highly specific electronic biosensors," *Proc.Natl.Acad.Sci. USA*, vol. 100, pp. 4984–4989, 2003.

[194] B. Mahar, C. Laslau, R. Yip, and Y. Sun, "Development of carbon nanotube-based sensors - a review," *IEEE Sensors Journal*, vol. 7, pp. 266-284 2007.

[195] Z. Liu, F. Galli, K. G. H. Janssen, L. Jiang, H. J. v. d. Linden, D. C. d. Geus, P. Voskamp, M. E. Kuil, R. C. L. Olsthoorn, T. H. Oosterkamp, T. Hankemeier, and J. P. Abrahams, "Stable Single-Walled Carbon Nanotube−Streptavidin Complex for Biorecognition," *J. Phys. Chem. C*, vol. 114, pp. 4345-4352, 2010.

[196] P. Weber, D. Ohlendorf, J. Wendoloski, and F. Salemme, "Structural origins of high-affinity biotin binding to streptavidin," *Science*, vol. 243, pp. 85-88 1989.

[197] *Streptavidin,http://en.wikipedia.org/wiki/Streptavidin*.

[198] *Streptavidin reagents, http://www.sigmaaldrich.com/life-science/cell-biology/antibodies/antibody-products.html?TablePage=9674497*.

[199] E. A. Bayer and M. Wilchek, "Biotin-binding proteins: Overview and prospects," *Methods in Enzymology*, vol. 184, pp. 49-51, 1990.

[200] Y. Cui, Q. Wei, H. Park, and C. M. Lieber, "Nanowire Nanosensors for Highly Sensitive and Selective Detection of Biological and Chemical Species," *Science*, vol. 293, pp. 1289-1292, 2001.

[201] F. Patolsky, G. Zheng, O. Hayden, M. Lakadamyali, X. Zhuang, and C. M. Lieber, "Electrical detection of single viruses," *PNAS*, vol. 101, pp. 14017-14022, 2004.
[202] E. Zheng, F. Patolsky, Y. Cui, W. U. Wang, and C. M. Lieber, "Multiplexed electrical detection of cancer markers with nanowire sensor arrays," *Nature Biotechnology*, vol. 23, pp. 1294 - 1301, 2005.